Detailed error budget analysis and simulations

Error terms

Error terms can be grouped in 4 categories:

1. Astrophysical noise

Includes stellar activity on the central star and astrometric wobble of background reference stars.

2. Fundamental measurement noise

Measurement noise due to the primary design parameters such as telescope diameter, pixel sampling and wavelength. This would be equal to the total instrument noise in the absence of defects in the detector or optical train.

Includes photon noise contribution from background stars and zodi background.

3. Static astrometric error terms

Contribution of all static defects, such as poorly calibrated detector response or manufacturing errors in the optical surfaces.

Even perfectly static defects produce astrometric errors, as the trajectories of the background stars on the focal plane are slightly different between observations (proper motion, parallax).

4. Dynamic astrometric error terms

Errors due to changes of the telescope and instrument between observations.

Includes variations in the shape of optics surfaces, variations in detector geometry (detector pixels move between observations) and variations in detector sensitivity.

Dynamic errors are not fully calibrated by the spikes (spikes have a limited SNR, and do not fully sample the field of view). Dynamic errors can also create errors in the measurement of the spikes positions.

Measurement noise

	Noise term	Description	Impact
Astrophysical noise	Sunspots and stellar activity	The central star photocenter moves due to stellar activity and sunspots, creating an astrometric signal	Small to moderate
	Astrometric signal of background reference stars.	Several background stars have astrometric motions due to multiplicity and planets	Small thanks to large number of background stars (averaging). Background stars are also distant and low metallicity (Halo stars)
Fundamental measurement noise	Photon noise on background stars	Photon noise limits the position measurement accuracy on faint stars. The faintest stars are below the zodiacal light level.	Dominant on faint stars
	Photon noise due to zodiacal light		
	Detector finite sampling of a polychromatic PSF	The position measurement error is somewhat larger than the photon-noise limit.	Small for Nyquist sampled image
	Detector readout noise		Small if exposure time is properly chosen
Static astrometric errors	Detector flat field, and sensitivity variations within pixels	These unknown errors produce errors in the position measurement of background stars. Thanks to their roll anticorrelation, they average down quickly with roll.	Small thanks to roll averaging
	Static astrometric distortion due to optics surface figure	Between observations, the trajectory of background stars moves slightly on the focal plane due to proper motion and parallax of the central star. This transforms static distortions into a small time-variable astrometric error.	Moderate to strong Can be mitigated by increasing total light in spikes, which allow (1) smaller spacing between spikes in focal plane, and (2) reduced impact of spike photon noise on the astrometric calibration
	Static astrometric distortion due to unknown detector geometry		
Dynamic astrometric errors	Dynamic astrometric distortion due to change in optics surface figure	Mirror shapes change between observations, and this distortion is not perfectly removed by the astrometric calibration using diffraction spikes	
	Dynamic astrometric distortion due to change in detector geometry	The large focal plane array is likely made of many individual chips which can move and deform. This distortion is not perfectly removed by the astrometric calibration using diffraction spikes.	
	Dynamic astrometric distorition due to change in detector response	Unknown changes in detector response are misidentified as a motion of the spikes, creating a change in the astrometric calibration	Significant if > 1%
	Dynamic astrometric distorition due to spots moving on mirror	Spots move on the PM between observations, creating a differential motion between spikes and background stars	Small ?

Approach

Baseline: 1.4-m telescope (PECO), with 0.25 sq deg FOV (0.5 x 0.5 deg)

The FOV is chosen to reach performance goals in a sufficiently stable system. Photon noise limited performance for this FOV is 0.044 μas single measurement at galactic pole, but actual performance is significantly lower (larger error) due to distortions and detector limits.

When detailed simulations are required, a smaller FOV system is used (0.1 deg radius = 0.03 sq deg FOV) to ease computations.

	Value in simulations	Value for mission	Rationale for flight instrument value	Impact on astrometric accuracy
Telescope diameter (D)	1.4 m		PECO sized, cost constrained	Astrometric accuracy goes as D^{-2}, thanks to larger collecting area and smaller PSF size (assuming constant FOV)
Detector pixel size	44 mas		Nyquist at 600 nm	Little impact as long as sampling is close to or finer than Nyquist
Field of view (FOV)	0.03 sq deg (0.1 deg radius)	0.25 sq deg (0.5 deg X 0.5 deg)	low WF error across field, 1.6 Gpix detector	Astrometric accuracy goes as $FOV^{-0.5}$
Single measurement time	48 hr		Typical single observation duration for coronagraph	Astrometric accuracy goes as $t^{-0.5}$
Dot coverage on PM (area)	1%	8%	Keeps thoughput loss moderate in coronagraph	Larger dot coverage allows observation of fainter sources.
Flat field error after calibration, static (high spatial frequency)	1.02% RMS, 6% peak		Conservative estimate for modern detector after calibration	Negligible effect on background PSF measurement (well averaged with roll)
Flat field error, dynamic	1e-4 RMS per pixel, uncorrelated spatially and temporally between observations		1e-4 loss in sensitivity for each pixel over 48 hrs = 2% per year = 10% over 5 yrs	Negligible effect on background PSF measurement, but significant effect on measurement of spikes locations
Telescope roll	1.0 rad (+/- 0.5 rad)		Manageable sunshielding	Larger telescope roll leads to better averaging of detector errors
Uncalibrated change in optics surface between observations for M2 & M3	40 pm		Wavefront measurement repeatability (optical element removed / reinserted) obtained when testing similar sized optics on ground	Larger change in optics surface reduces astrometric accuracy
Static optics surface errror (M3 mirror)	1.5 nm		WF error and PSD taken from similar existing optical element	Small impact on performance, as background PSFs are almost fixed between observations
Astrometric accuracy, single measurement, single axis, m_V=3.7, galactic pole	***0.58 µas***	***0.20 µas***	***0.2 µas is required to achieve science goals***	

Simulation description

Simulation assumes:

- 1.4m telescope TMA (Woodruff design)
- 1.5nm surface (3nm WF) optics for M2 and M3, PSD provided by Tinsley
- Circular field of view, 0.2 deg diam (0.03 sq deg)
- Galactic pole observation (worst case scenario)
- central star is m_V=3.7 (faintest of the 7 PECO targets for which an Earth can be imaged in <6hr, 14th brightest target in the 20 high priority targets list)
- 90% detector peak QE, 80% optical throughput (0.96^3 for optics reflectivity x 0.92 due to dots on PM)
- Nyquist sampled detector at 0.6 micron = 44 mas pixels
- Telescope roll = 1 rad (larger angle = better averaging, but more difficult to maintain stability)
- Single epoch observation = 2 day

Distortions in the system are computed with 3D raytracing (code written in C, agreement with Code V results from Woodruff has been checked)
Images produced by Fourier transform, and then distorted according to geometrical optics. Image sizes are 16k x 16k.

Numerical simulation approach

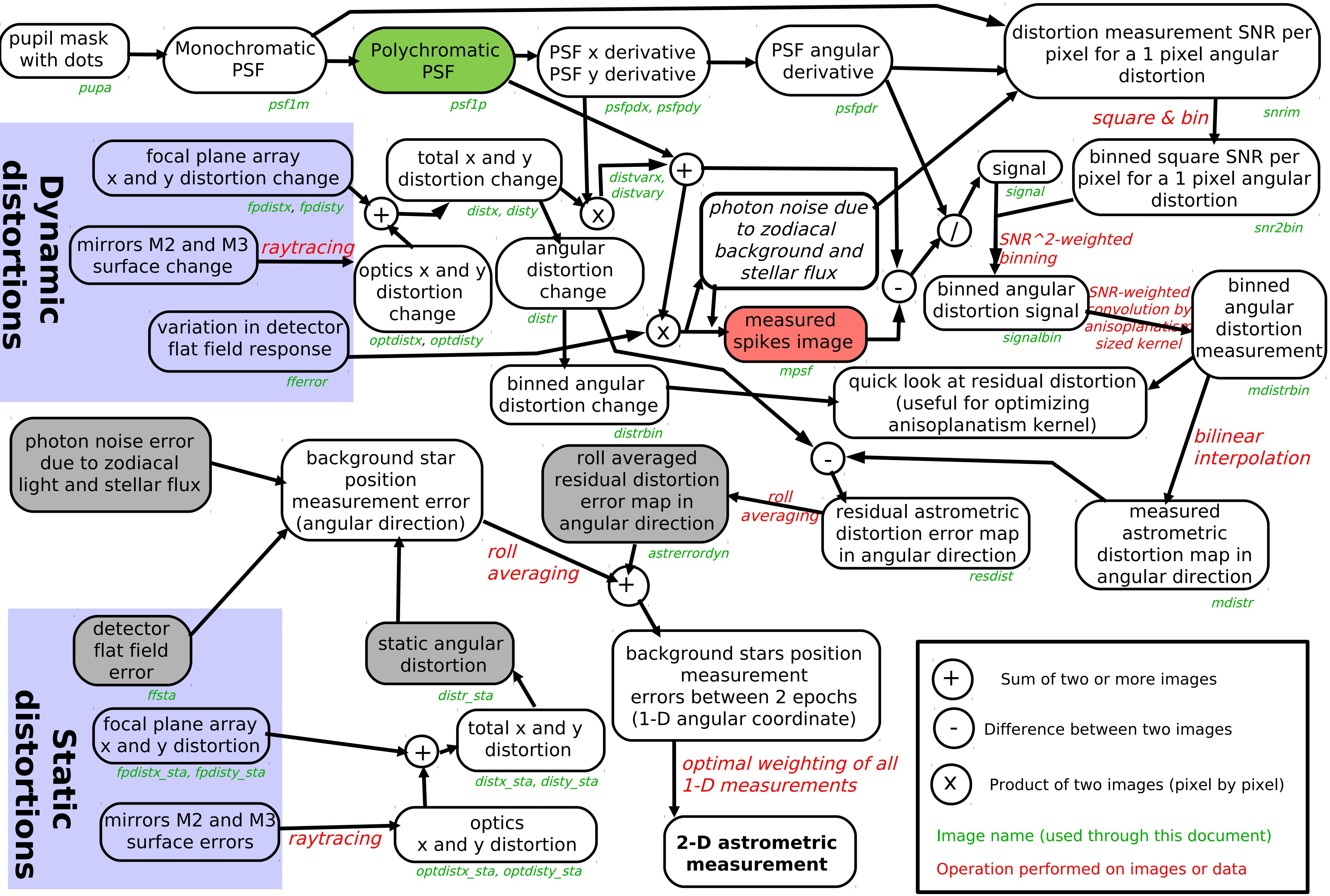

Simulation details

This series of slides describes in more detail each step of the numerical simulation. A red square is shown in the overal simulation description diagram to indicate which part of the simulation is being described.

Green text label next to boxes show the image or file name used in the source code, to help read the source code.

Numerical simulation approach

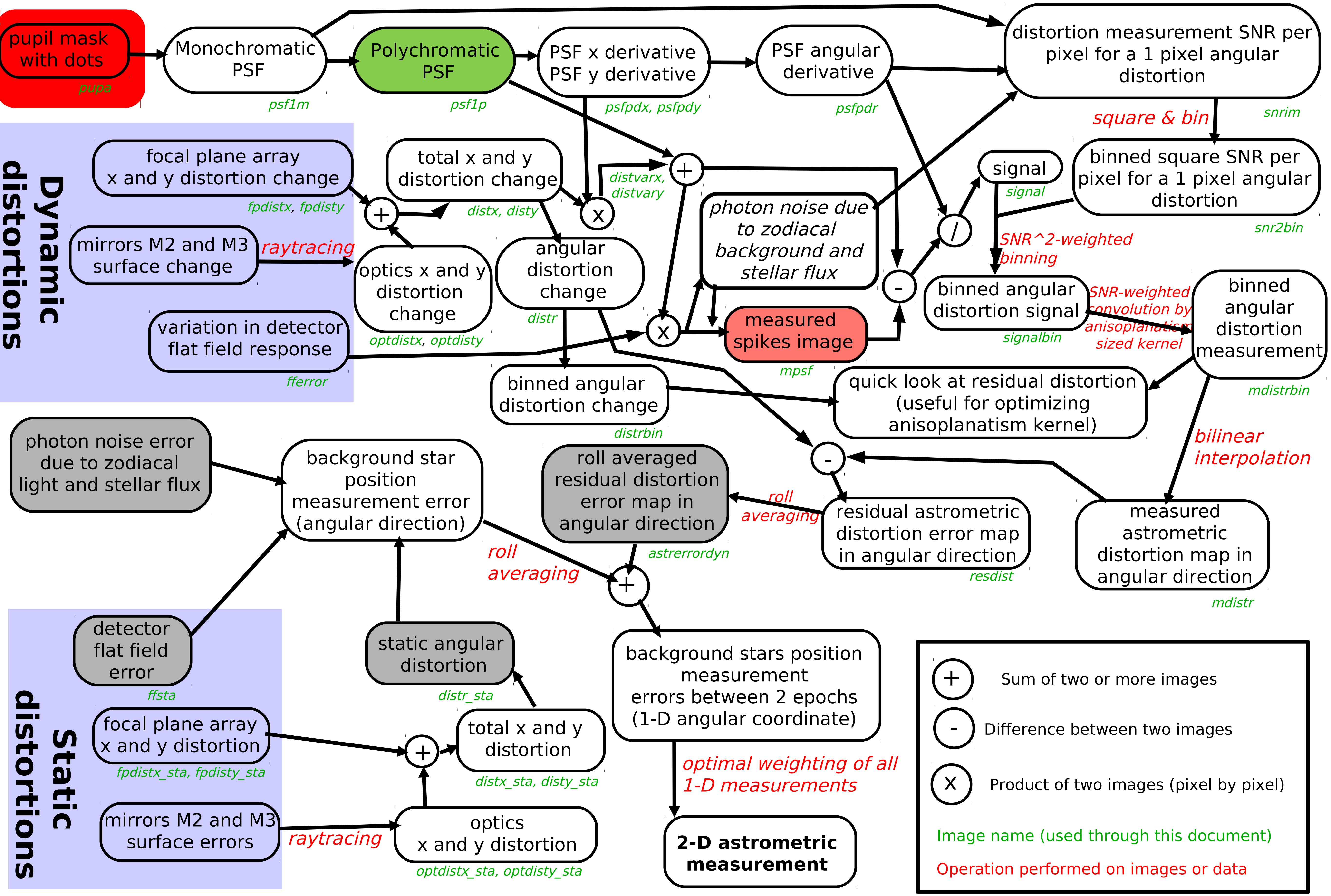

PM mask

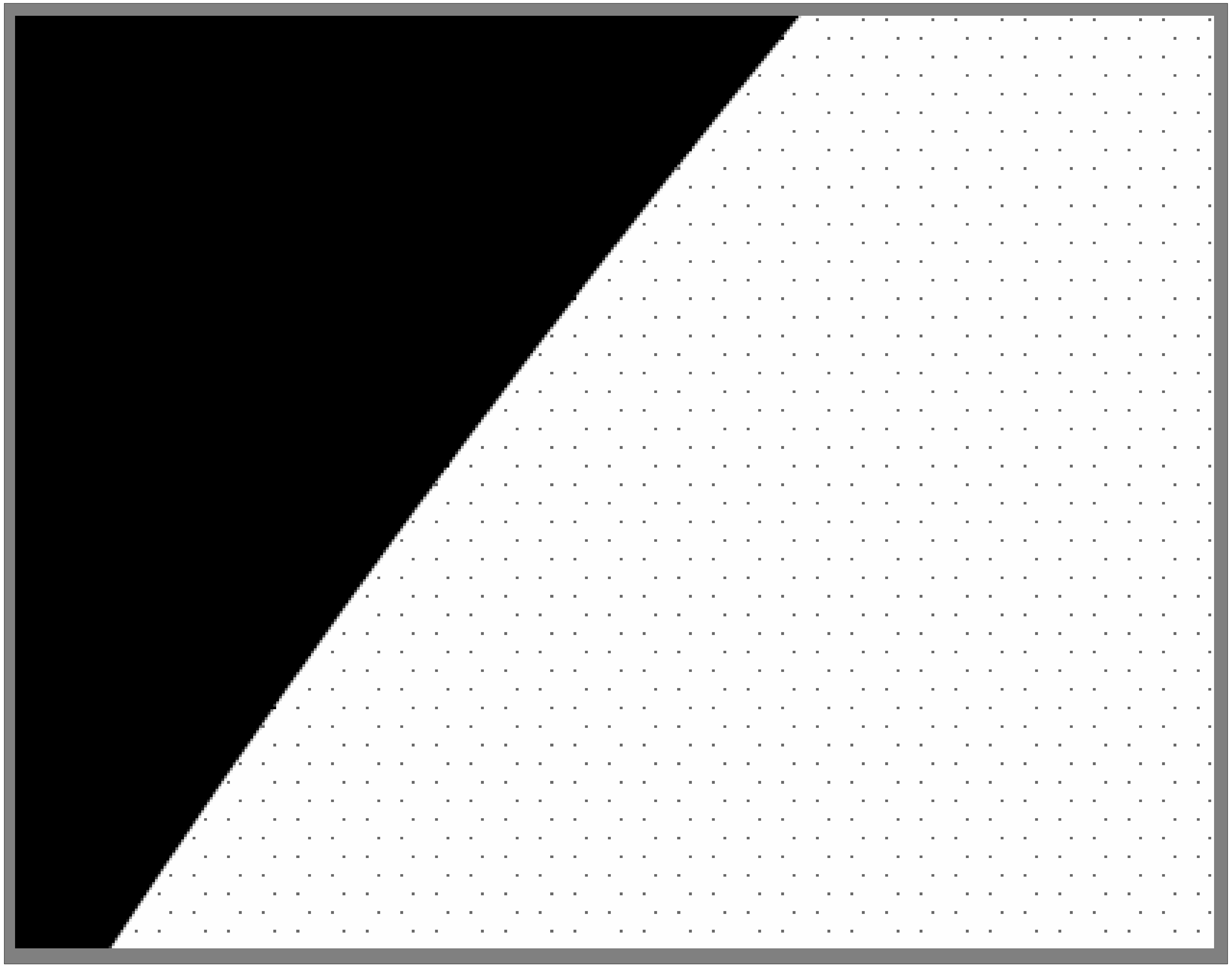

Hexagonal pattern dots. Dots cover 1% of PM surface. Dots are assumed to be perfectly placed, all with same size.

1/2 diameter of hexagon = 2.8 mm = distance between closest dots.
Dot diameter = 180 um

[note: for mission, dot diameter = 72 um; spacing = 0.5 mm]

Dots are assumed to be totally black.
Dots do not affect coronagraph if they are regularly spaced (no low spatial frequency)

Numerical simulation approach

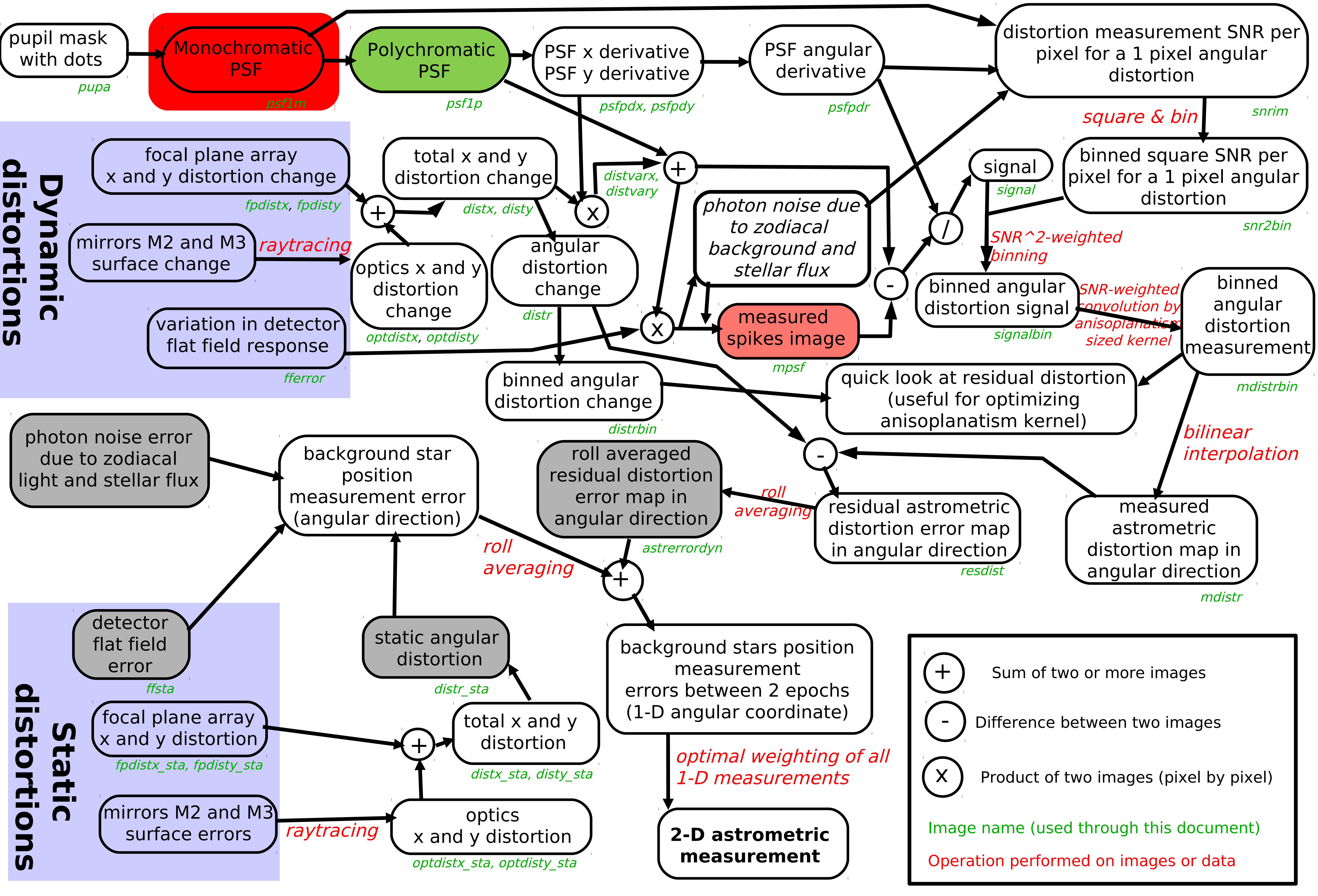

Monochromatic PSF

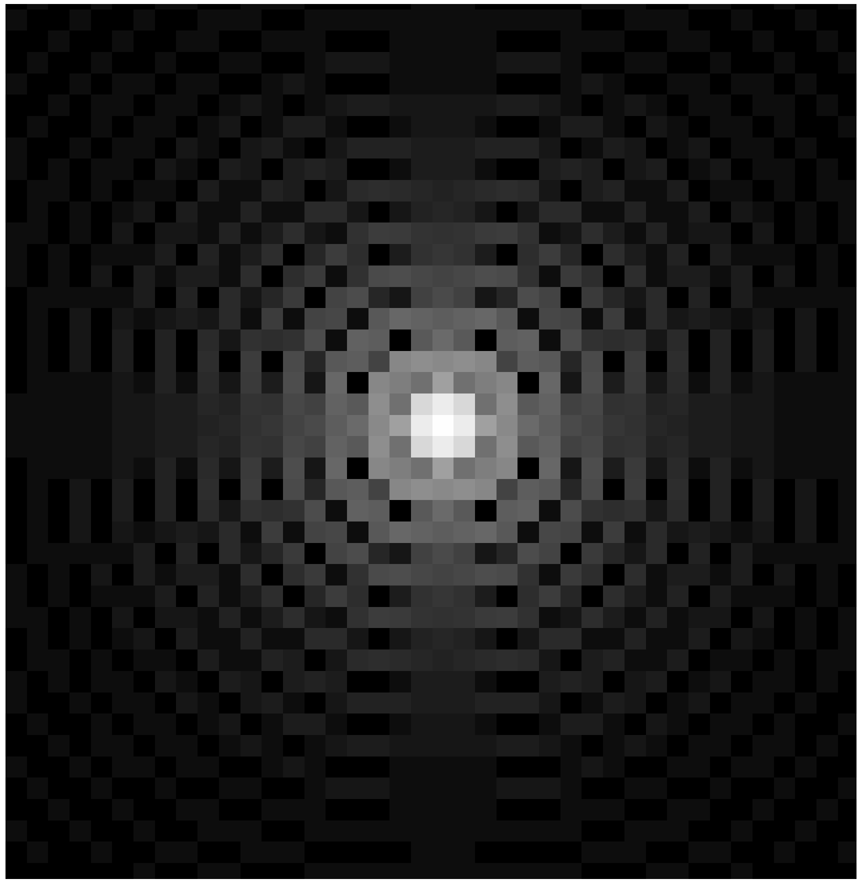

Central part of PSF is not disturbed by dots

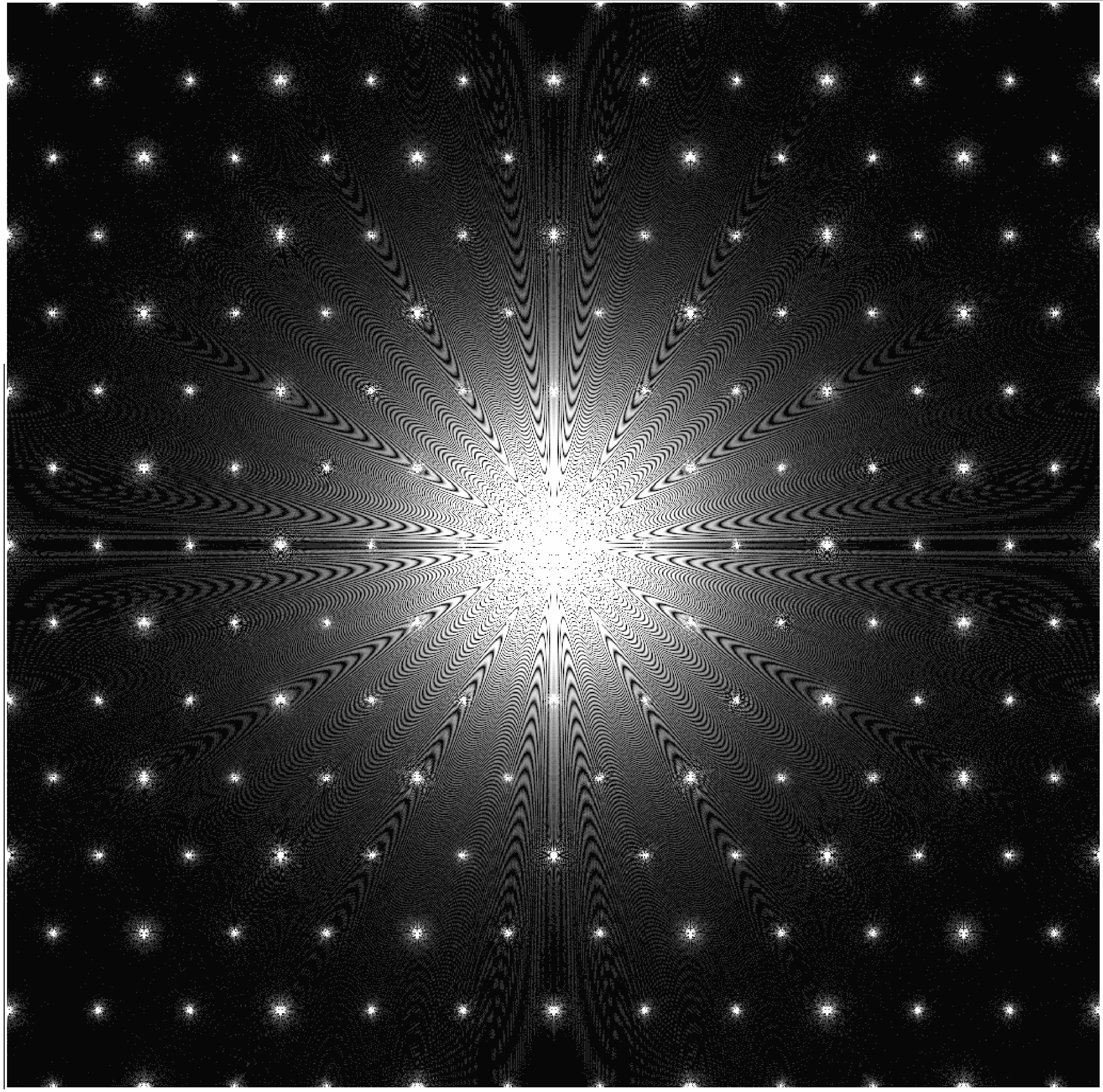

Full field PSF (0.2 deg on a side) shows 2D grid of diffraction orders

Numerical simulation approach

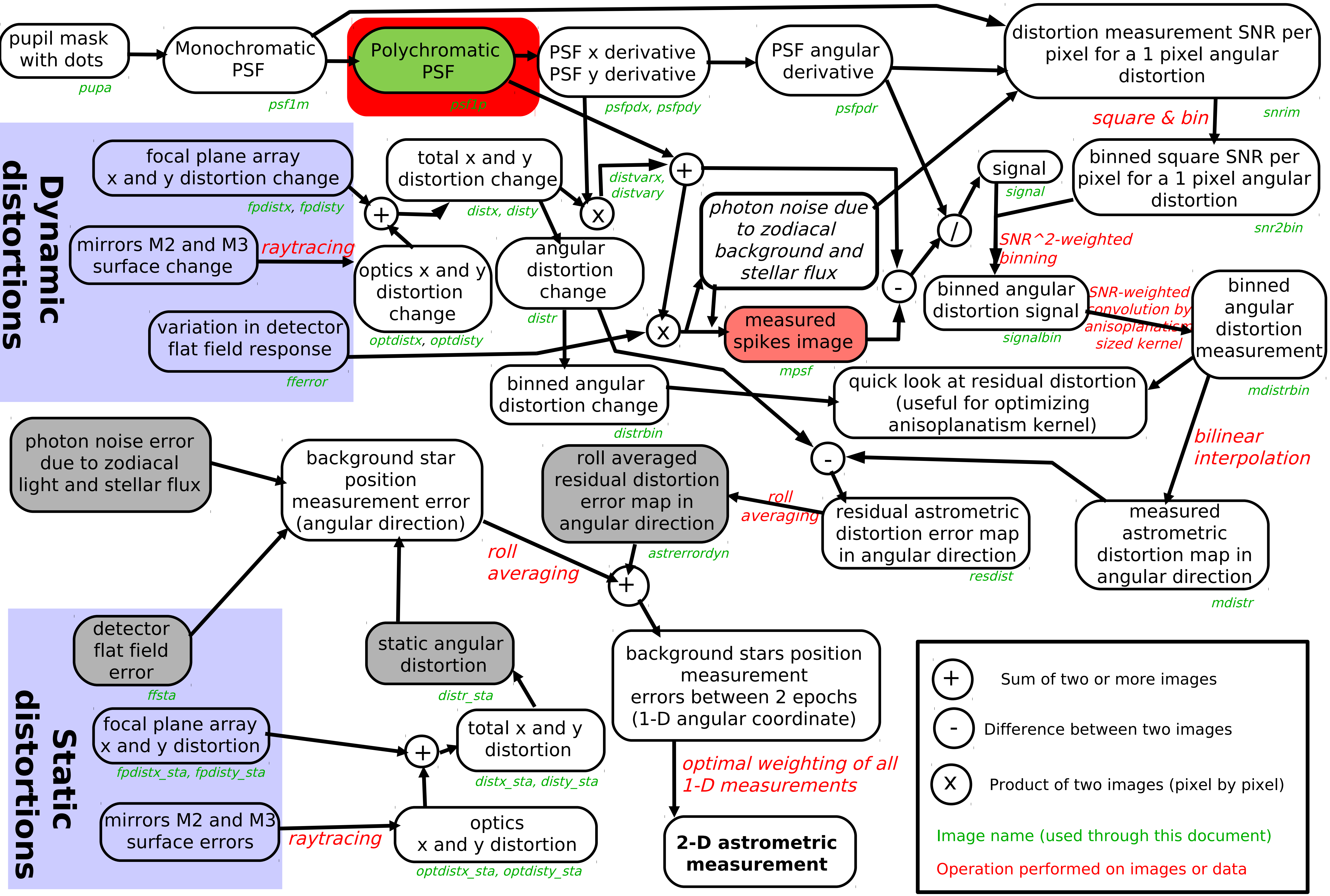

Polychromatic PSF

Computed as incoherent sum of 5000 monochromatic PSFs: 50 individual FFTs x 100 radial stretch steps

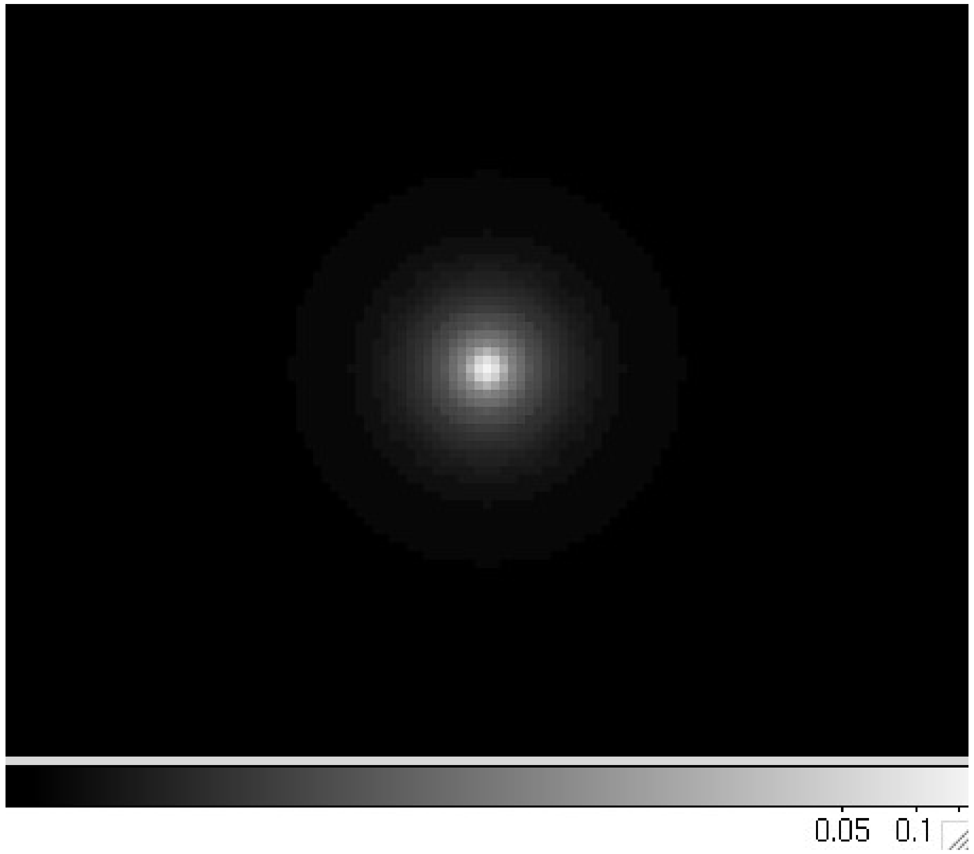

Central part of PSF

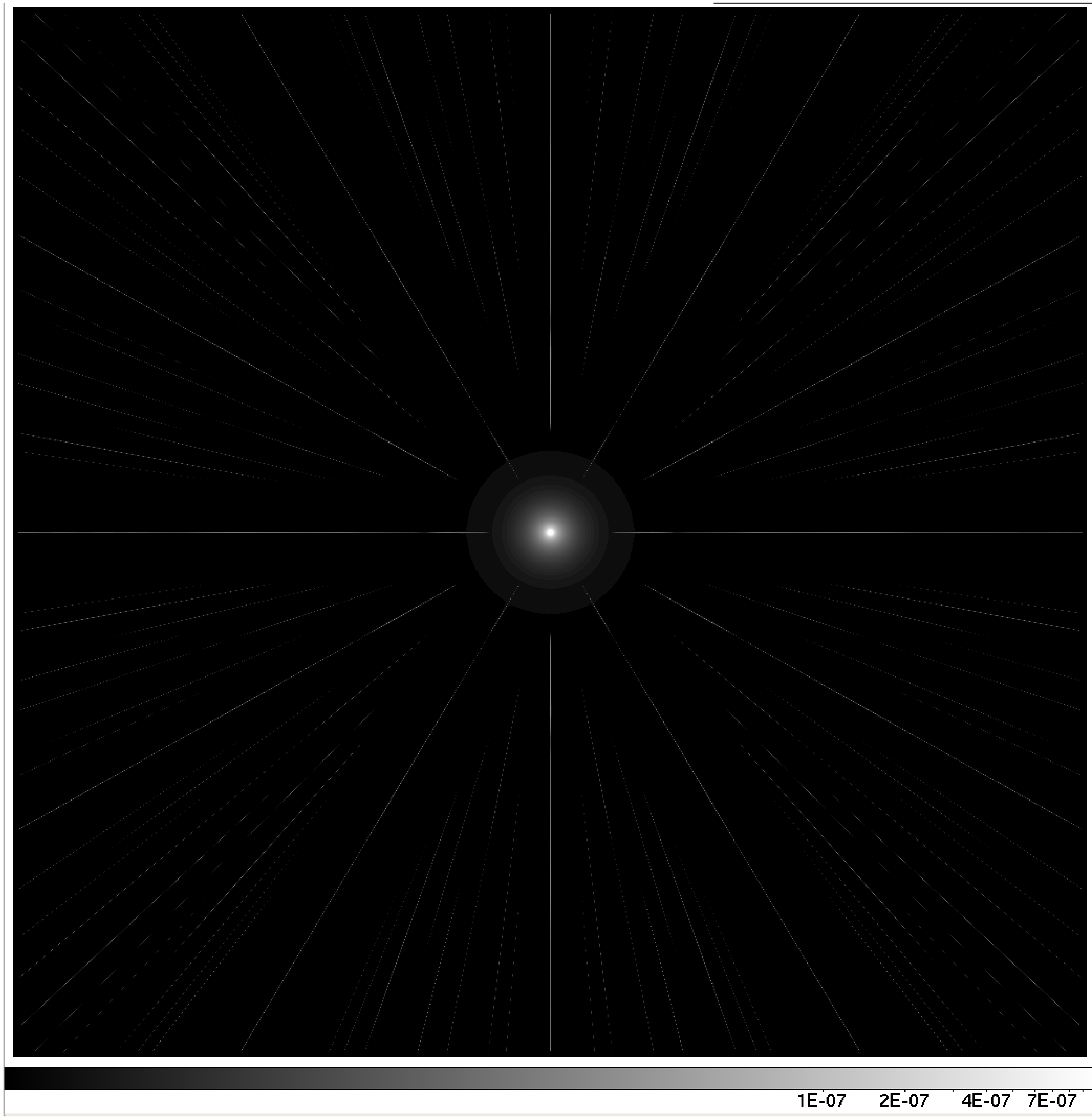

Full field PSF (0.2 deg on a side) shows thin narrow spikes

Polychromatic PSF

Brightest part of spikes is ~1e-7 of central PSF peak
Over most of the field, surface brightness is dominated by zodiacal light, not by spikes.

Scattering by PM surface roughness is much fainter than the spikes, as spikes diffract ~1% of starlight.

Central pixel has 17% of total flux

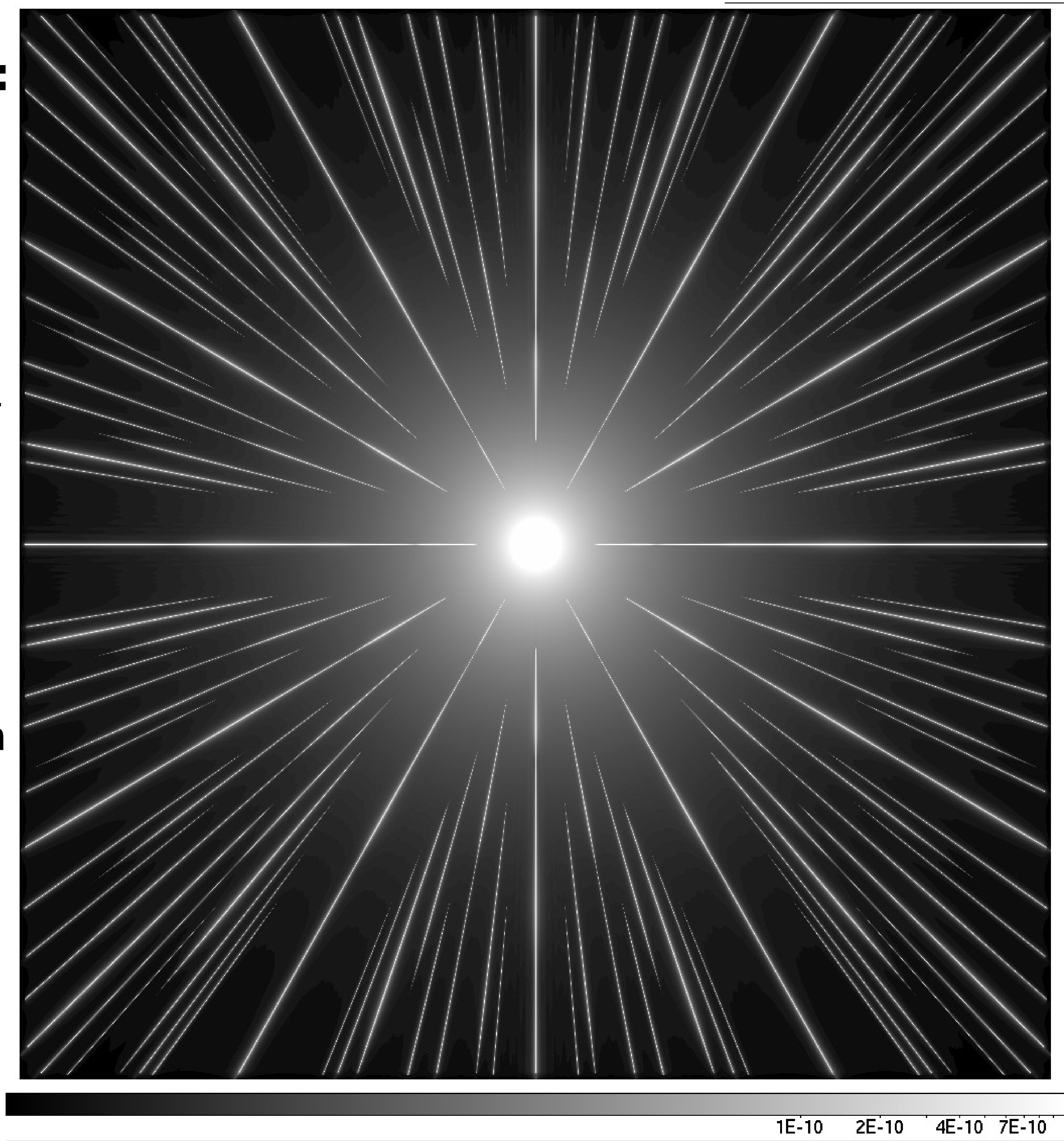

0.2 deg field PSF, log scale

Static distortions

Definition: Any error static through the mission lifetime.

Why do purely static errors matter ?

Background PSFs follow different trajectories during the telescope roll for different observation epochs. The trajectories are close (~arcsecond level), so what matters is the differential astrometric distortion over a ~1” distance.

Main errors:

- Distortions due to optical figure of mirrors M2 and M3
- Focal plane array geometry: position of individual detector chip & variations in pixel size across the detector
- Non-calibrated flat field errors

Impact and mitigation:

Static errors are not calibrated by the diffraction spikes:

- lack of absolute reference for spikes makes it impossible to calibrate static errors (where should the spikes be in a perfect system ?)
- spikes can only calibrate low order distortions, but relevant static errors are small scale errors

Numerical simulation approach

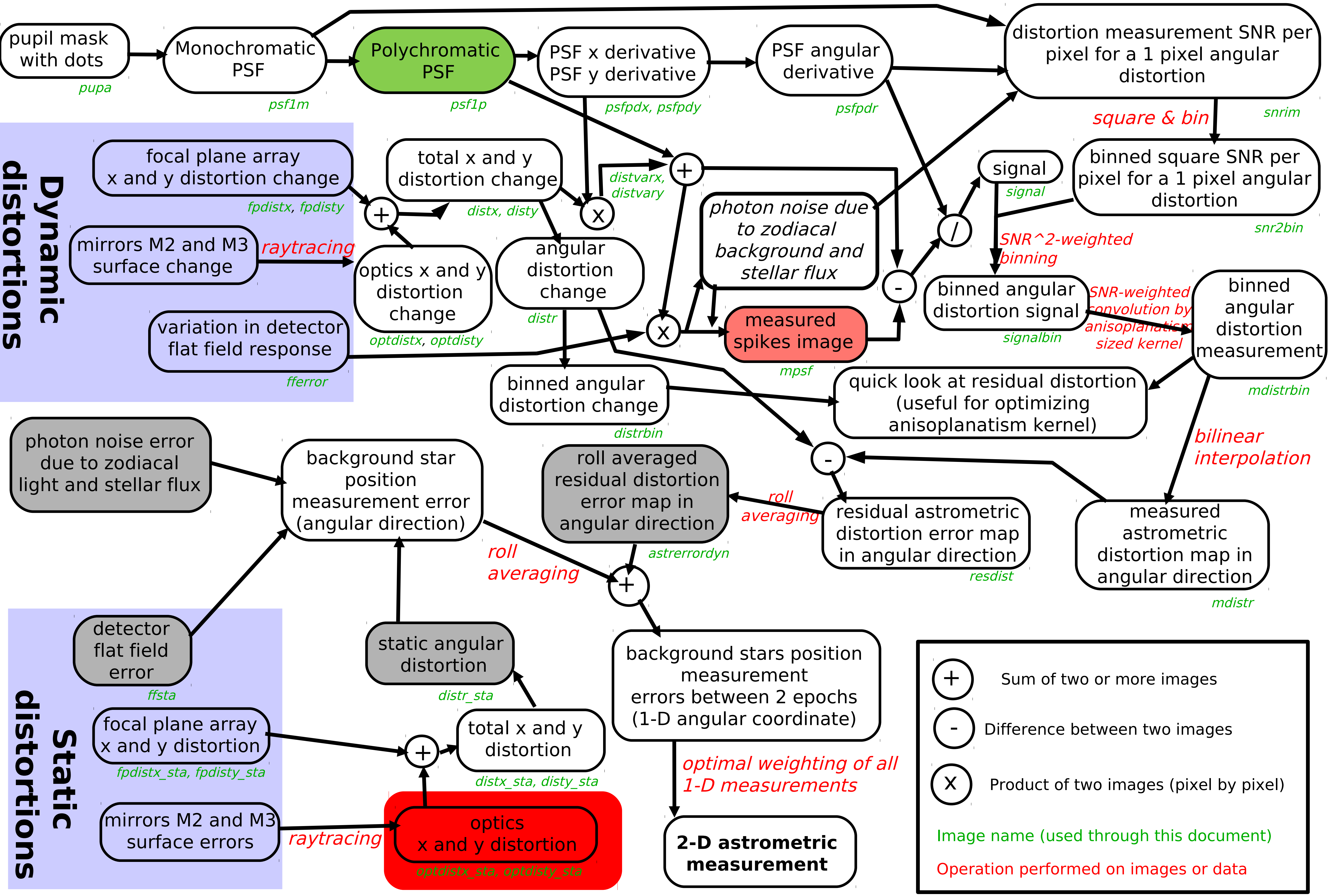

Static distortion map due to M2 & M3 optical surfaces

Distortion maps shown below is for 0.46x0.46 deg field. Unit is arcsec; left map is x, right map is y. Distortion is computed at 120000 positions on the sky, then interpolation is used to compute the full map.

Distortion amplitude is ~1 mas, dominated by low order modes. The differential distortion over ~1” is much smaller.

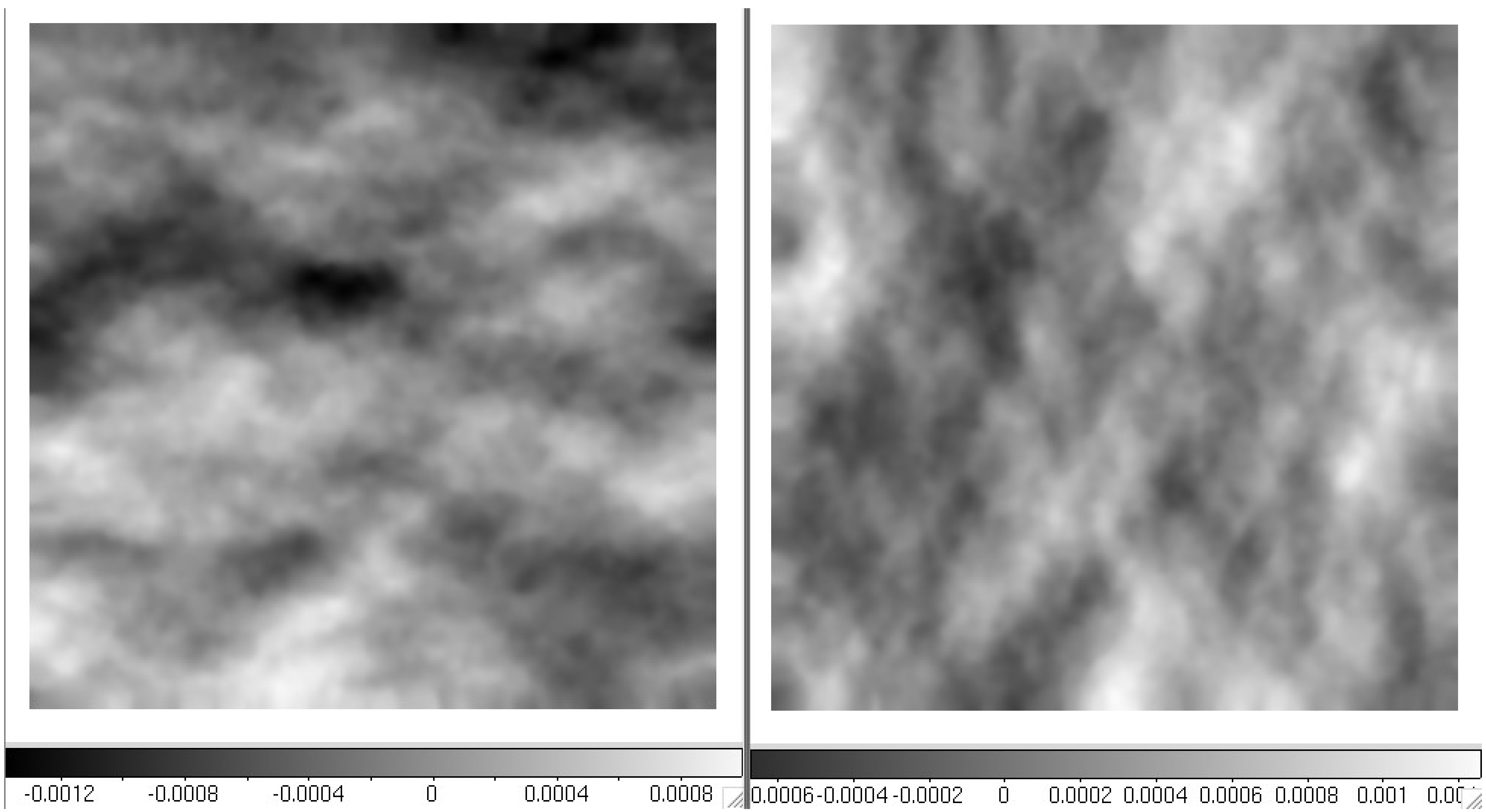

Numerical simulation approach

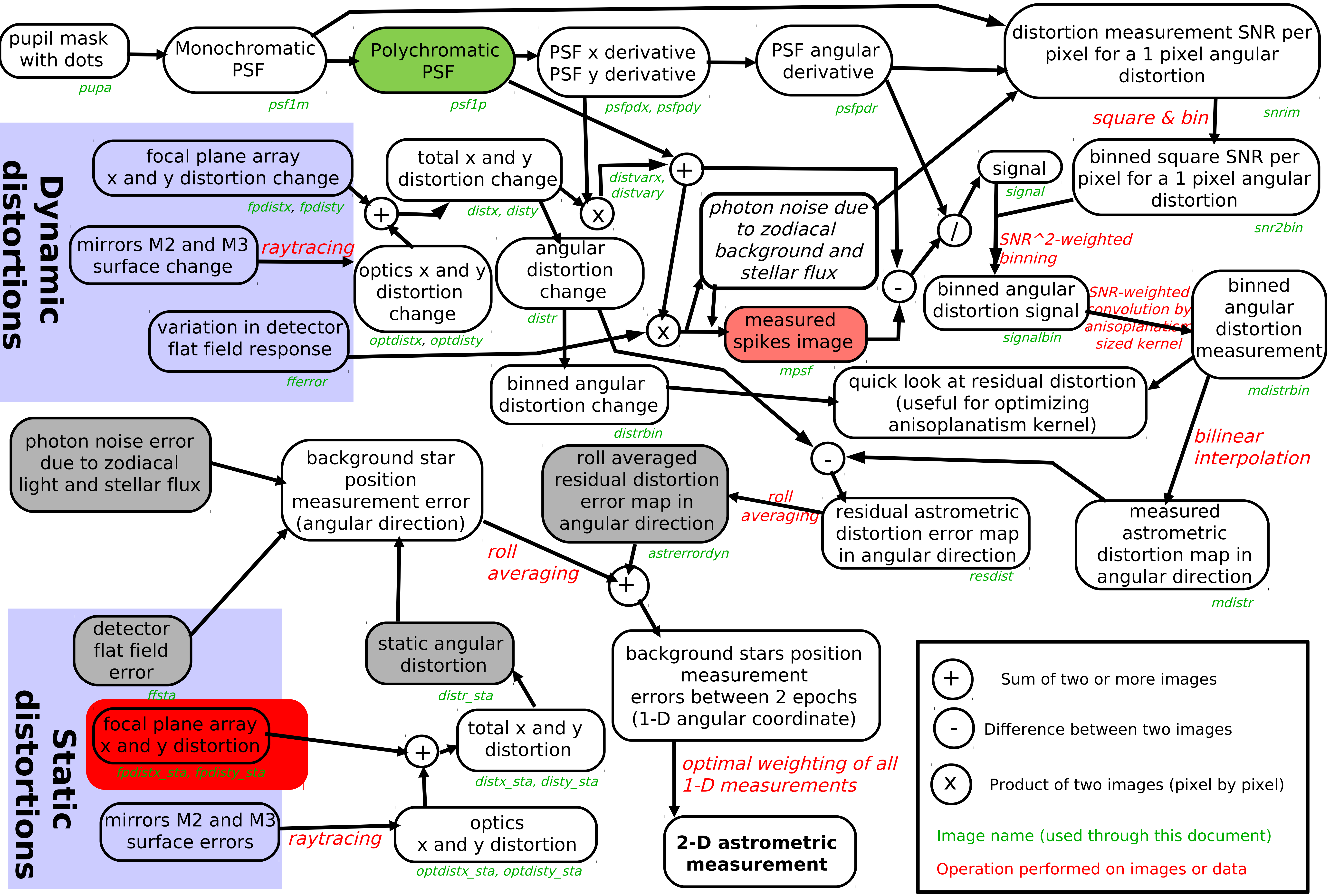

Static distortion map due to focal plane array

Distortion maps shown for 0.2 x 0.2 deg. Due to pixel size non-uniformity residual after ground/in orbit calibration of detector. Spatial frequencies chosen here put most power in between spikes and at ~arcsec separation (worst case)

~2/1000 pixel amplitude = 90 uas

left: x, right: y. Unit = pixel (44mas)

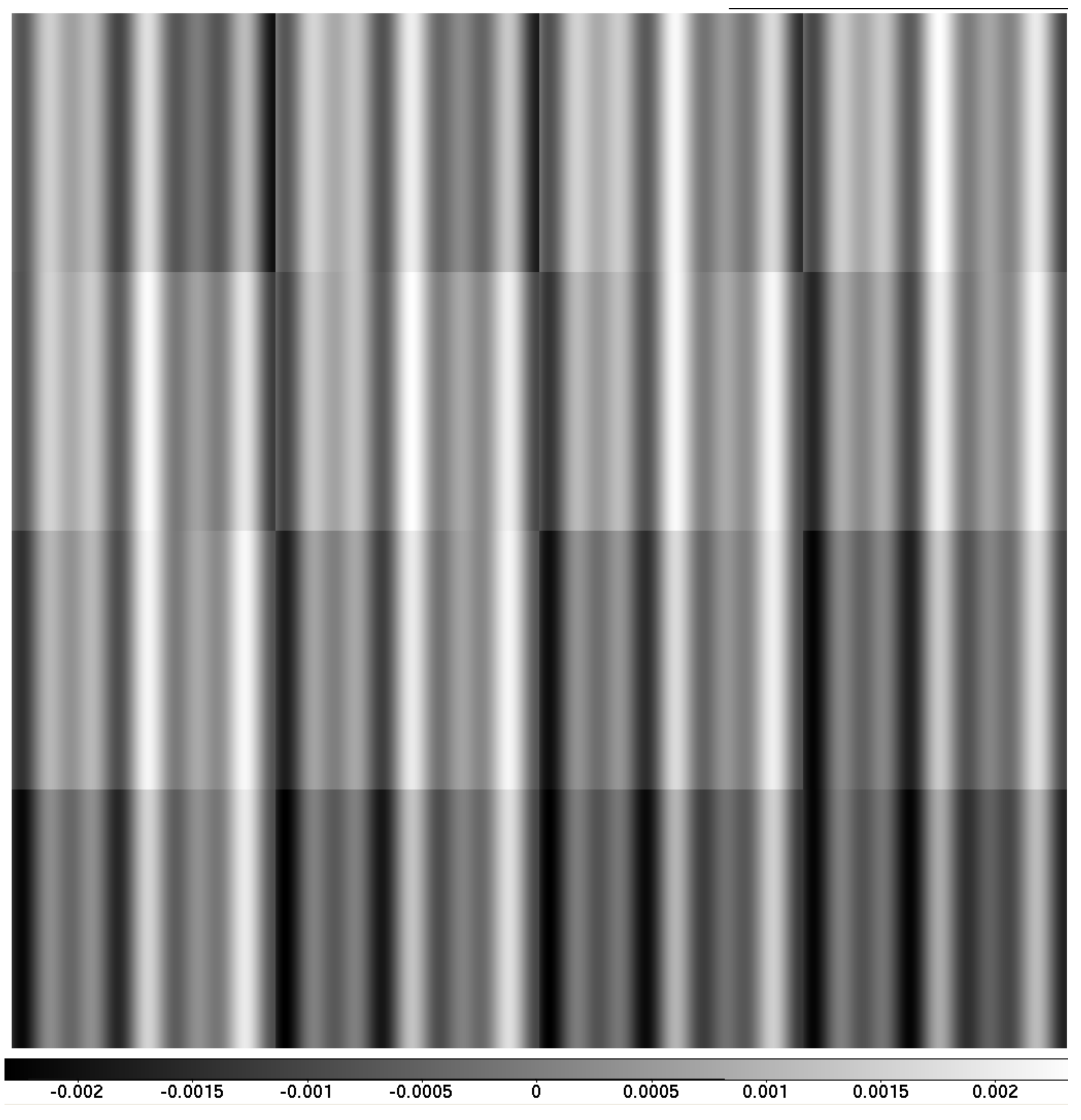

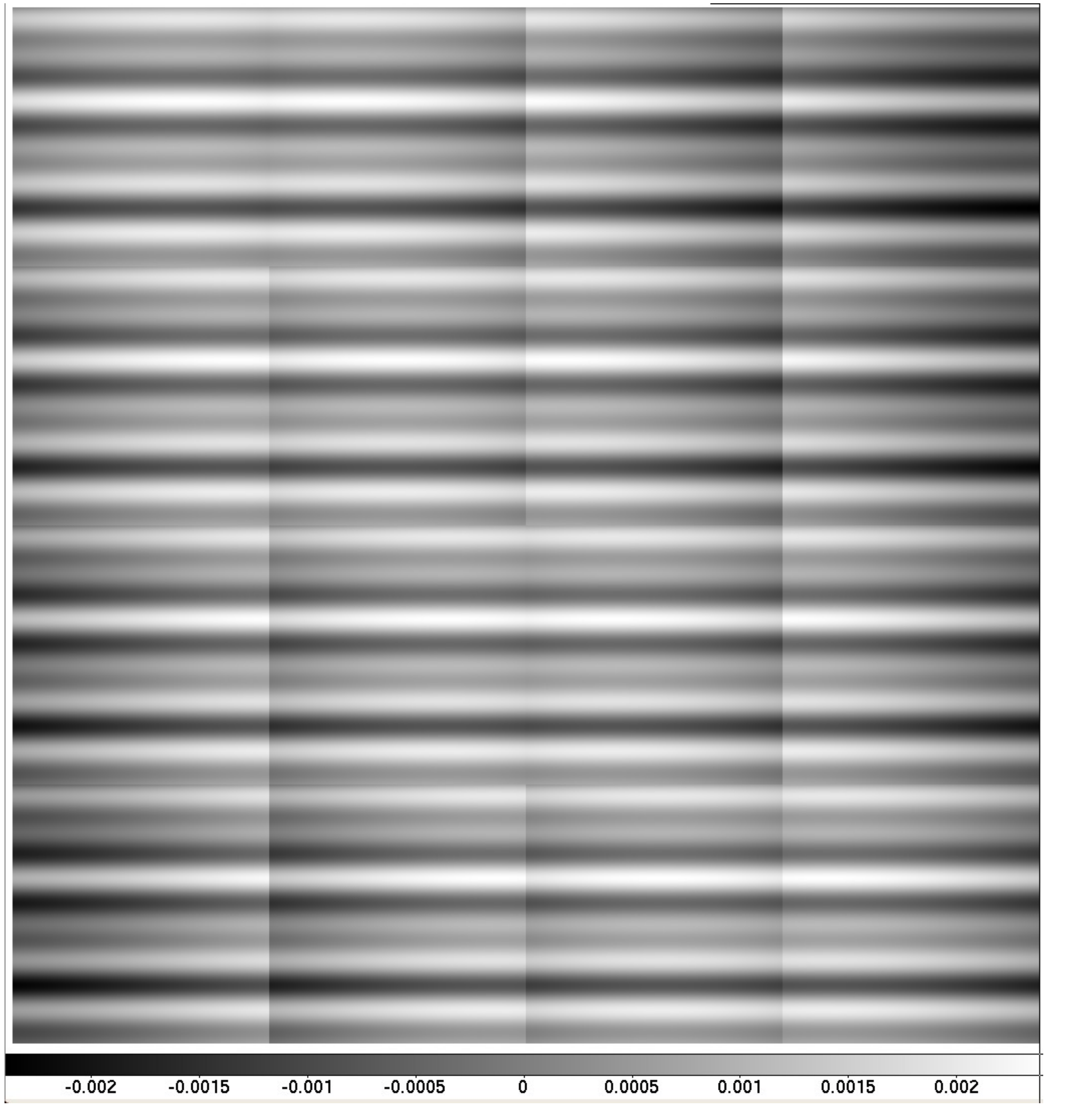

Numerical simulation approach

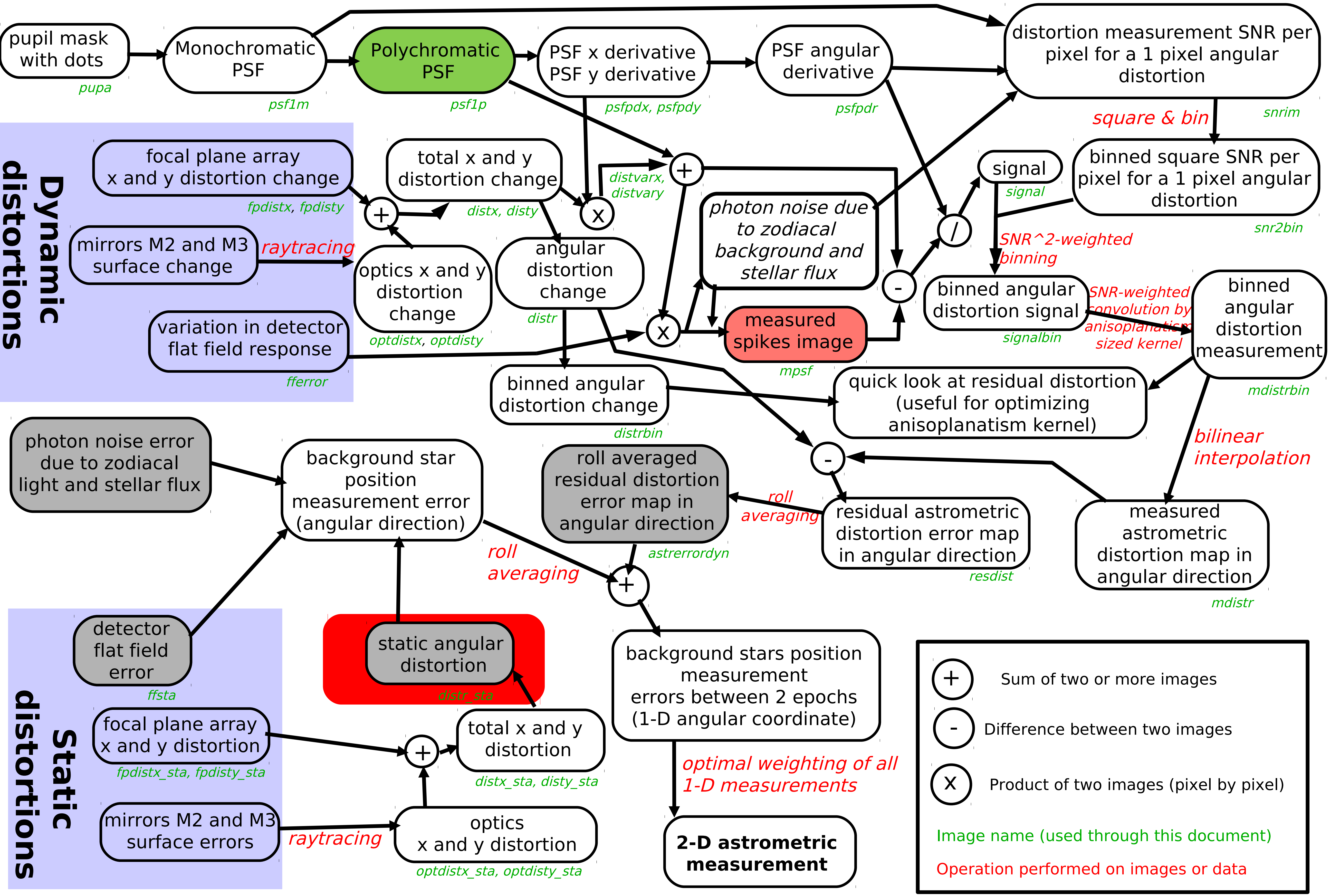

Total static distortion map

Angular coordinate distortion
(perp. to spikes)
map shown for 0.2 x 0.2 deg.
Unit = pixel (44mas)

distortion is +/- 1 mas approximately

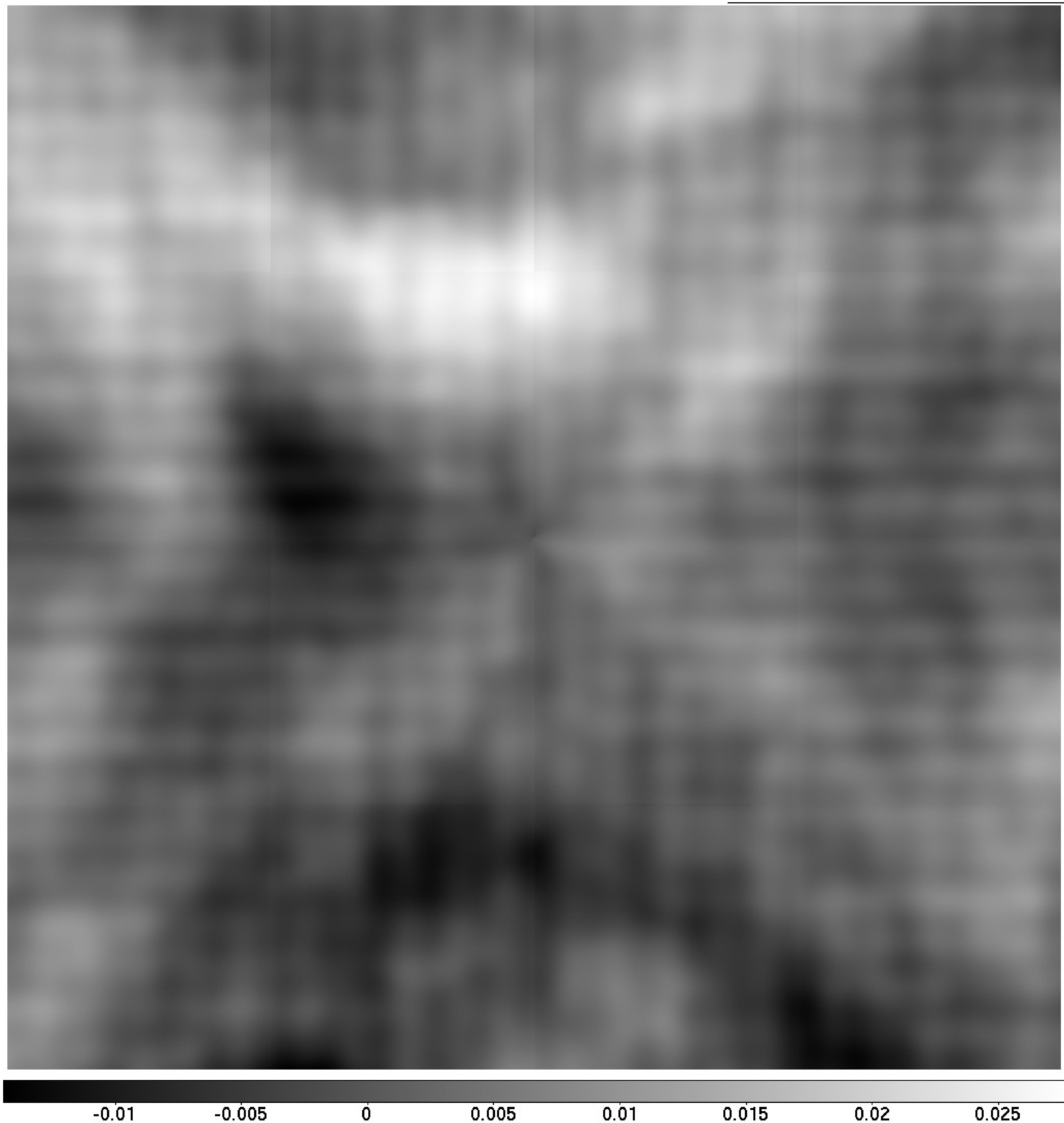

Numerical simulation approach

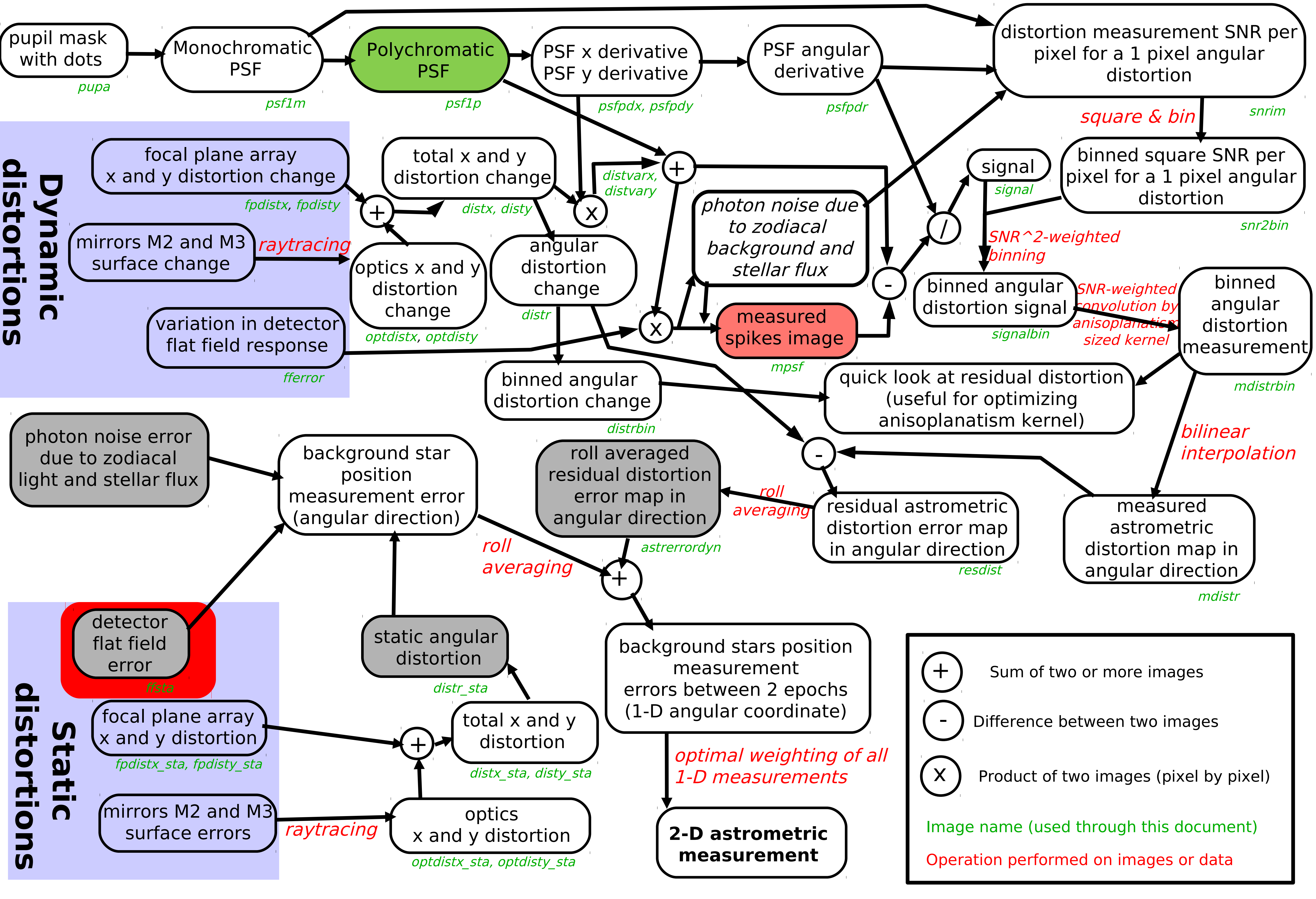

Static uncalibrated flat field error

1% random error + lines and columns errors
error is +/-6% peak, 1.02% RMS

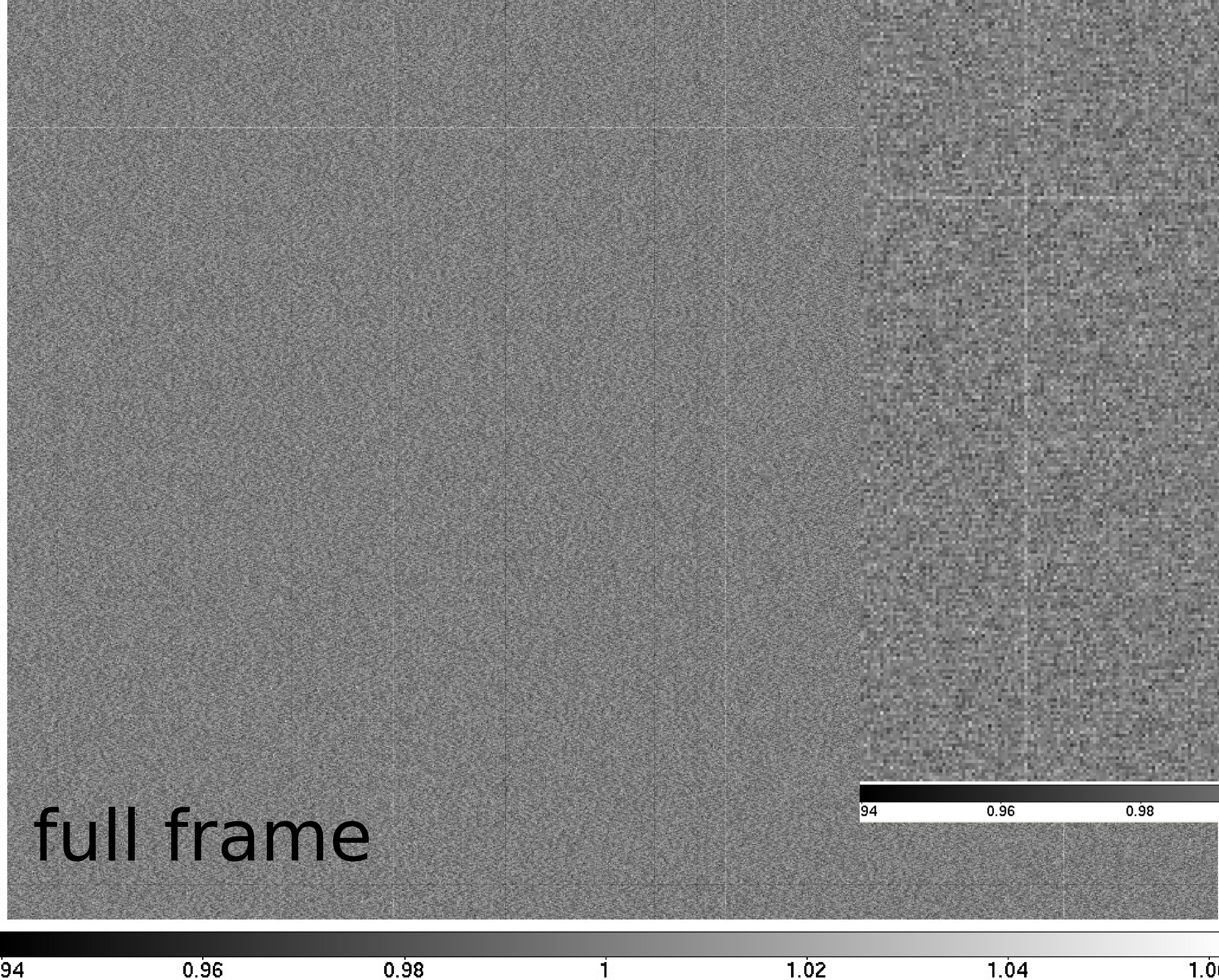

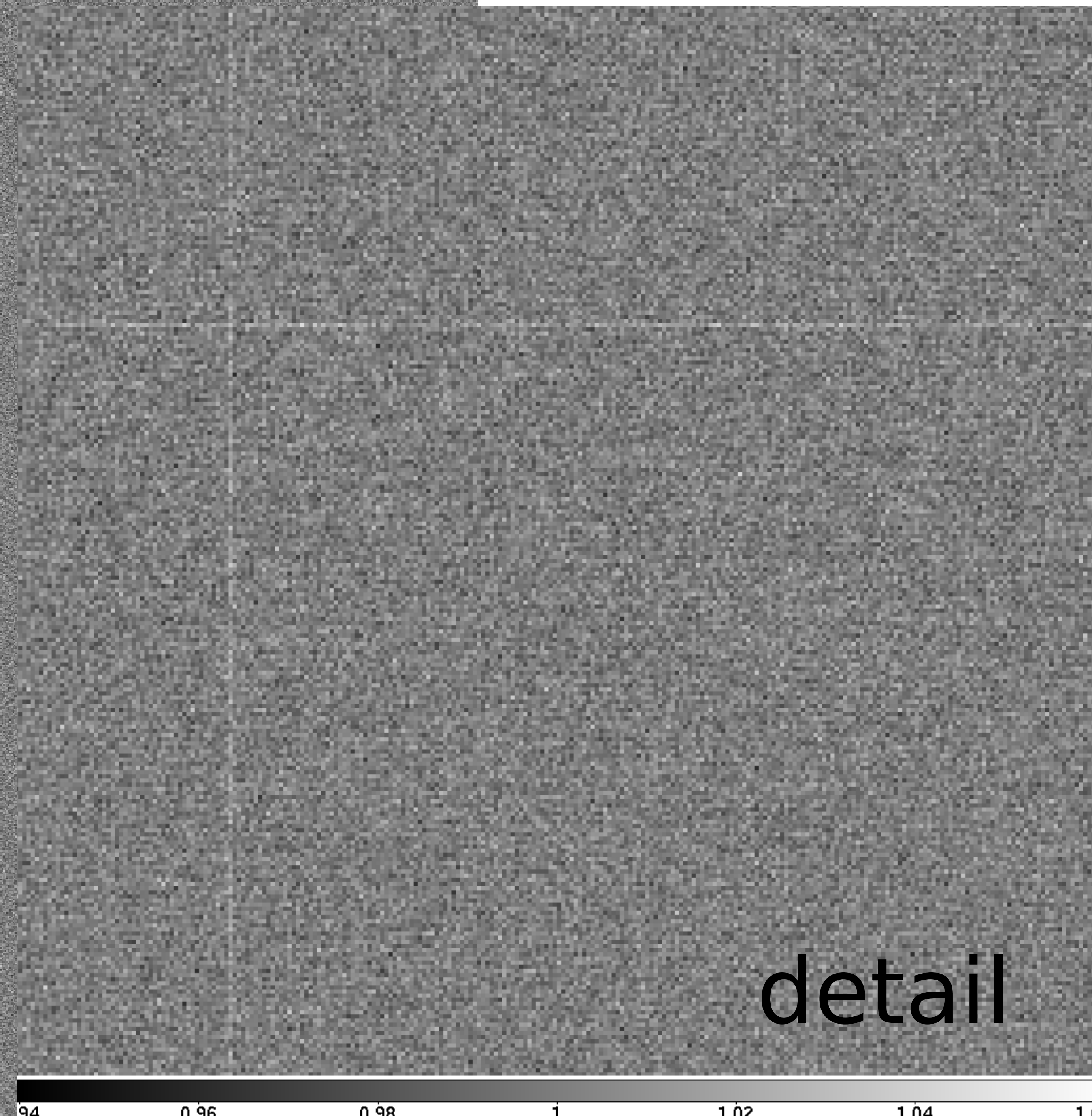

Flat field knowledge requirement

- With 0.2 deg diam, 1 rad roll, measurement is done over ~100 stars x 3000 independent positions (separated by more than l/D) on the detector = 3e5 measurements
- 0.2 uas = 1/200000 pixel -> allowed error (if not correlation) is <1/500 pixel ~ 1% error on flat field at small scales (pixel to pixel)
- Astrometric error due to pixel-to-pixel flat field errors is strongly anticorrelated along the PSF track on the detector-> averages closer to 1/N than 1/sqrt(N) -> flat field knowledge errors of a few % should be OK (see next slides)

Detector static errors are expected to be very small in the roll-averaged angular coordinate

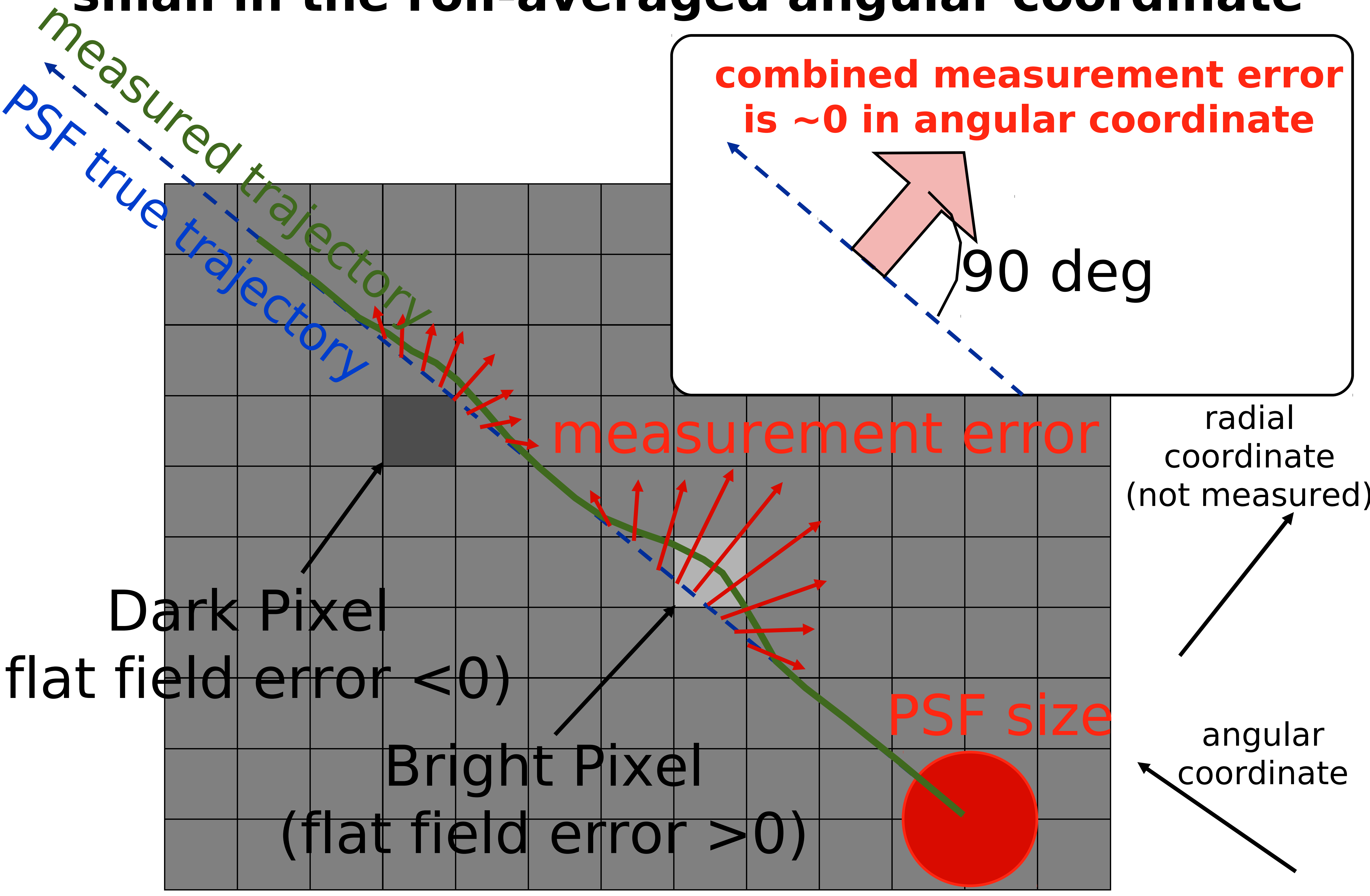

Numerical simulation approach

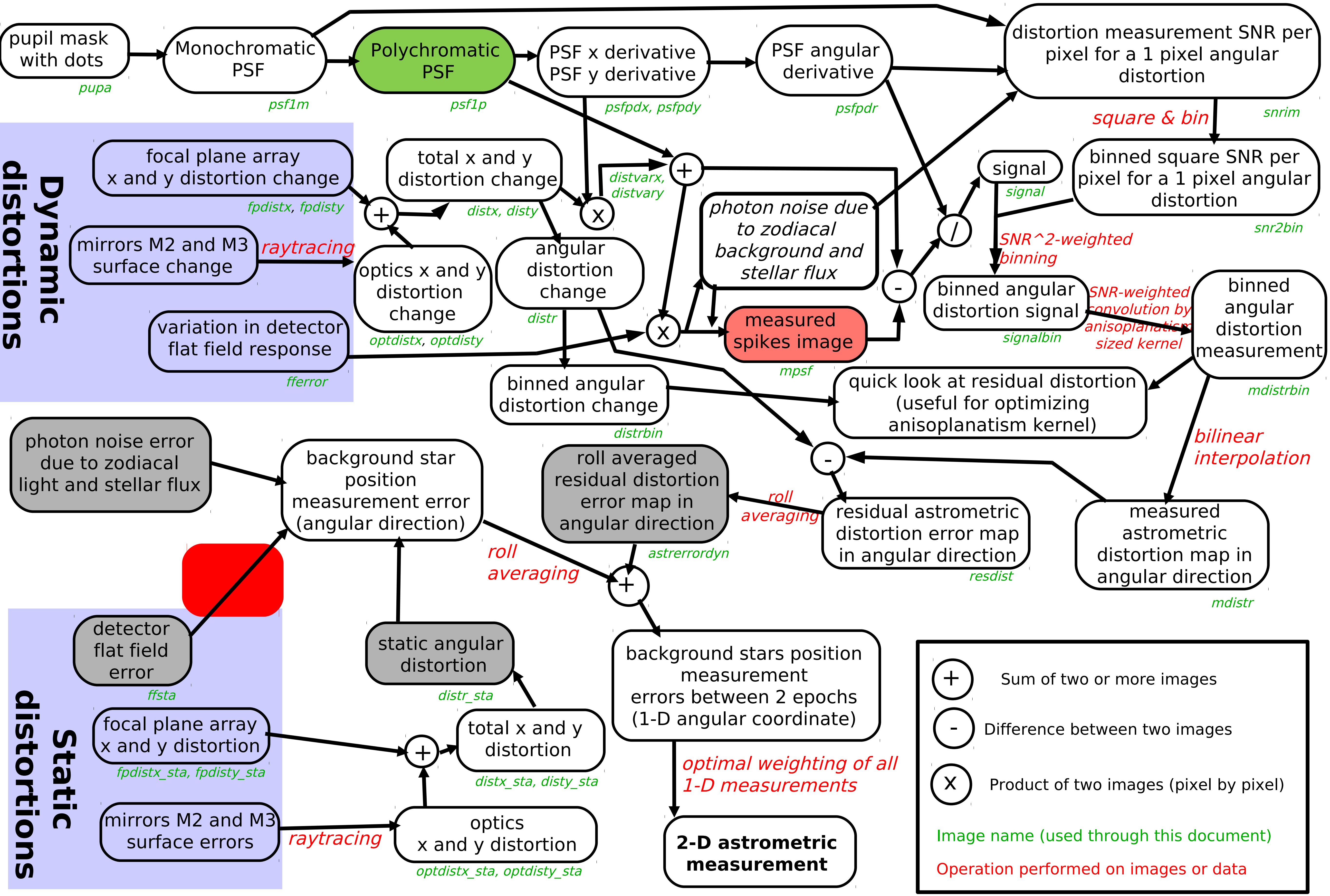

Numerical simulation of astrometric error due to flat field errors

Step 1: pre-compute how a single pixel sensitivity error “pulls” the estimated PSF position (= astrometric error kernel for a single pixel error). This is done at 0.1 l/D step size, over 10 l/D radius: for each 2-D offset (within 10 l/D radius, with 0.1 l/D step) between the PSF center location and the “bad” pixel, compute the error in PSF position measurement in x and y. Computation uses finely sampled PSFs binned down to the detector sampling.

Maps on the right show how a sensitivity error in a single pixel affects the PSF position measurement.

Maps are normalized to the relative pixel sensitivity error. Unit is l/D. Peak value is 0.05: a 1% sensitivity error can move the PSF measured position by 0.0005 l/D = 44 uas

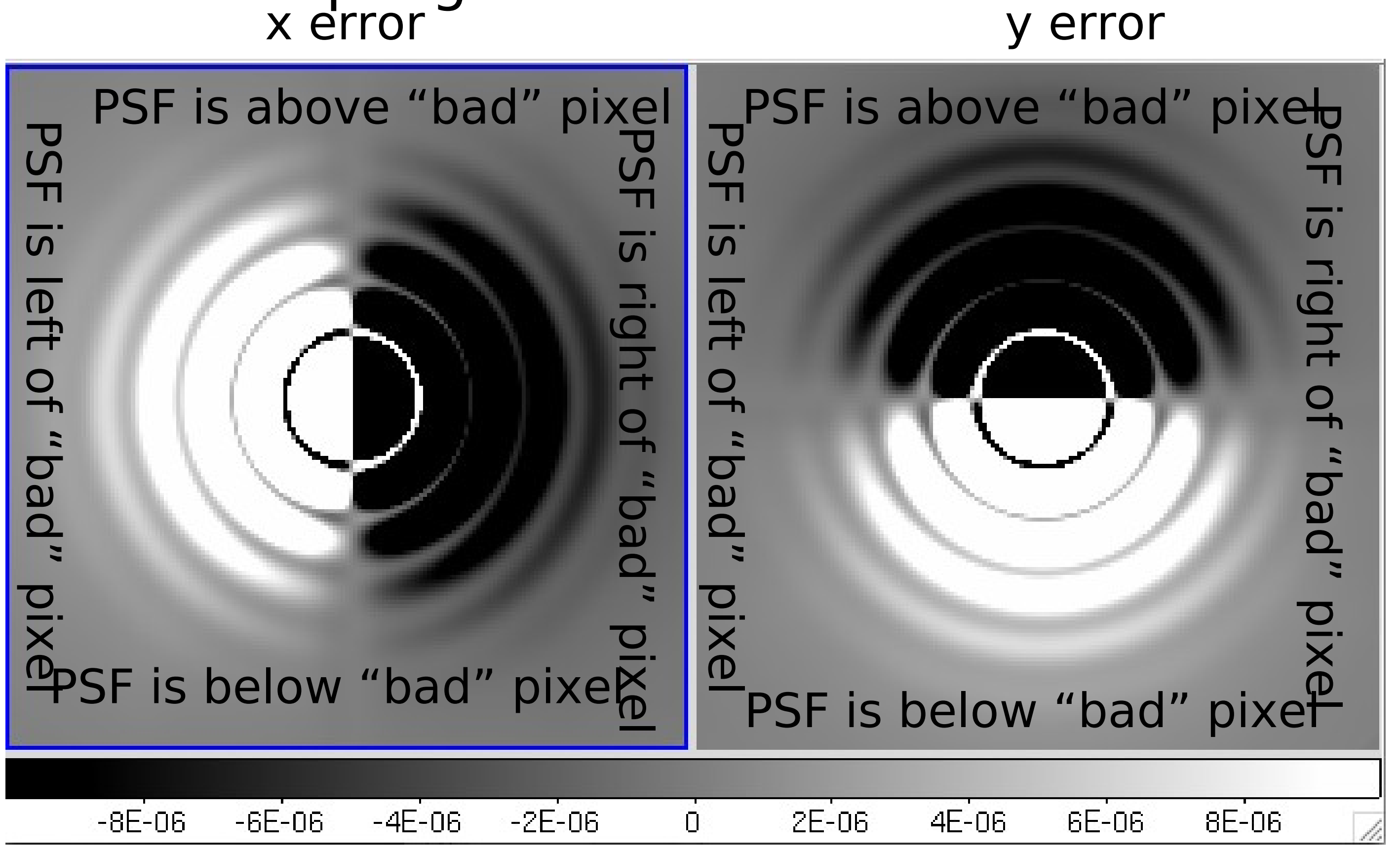

Step 2: For each roll angle and star, compute 2-D PSF position error by summing all errors due to pixels sensitivity errors within a 10 l/D radius of actual PSF position. This computation uses the maps shown above: for each pixel, the fractional offset between the pixel and the PSF is computed, and the corresponding error values (x and y) are derived from bilinear interpolation of the maps computed in step 1.

Flat field errors are strongly anticorrelated with roll angle -> they average as 1/N instead of 1/sqrt(N)

Figure on the left shows 1-D astrometric error for a single star as a function of roll angle.
The raw error (brown) is ~1e-3 l/D RMS (~0.1 mas).
The roll-averaged error (red) goes as 1/roll angle.

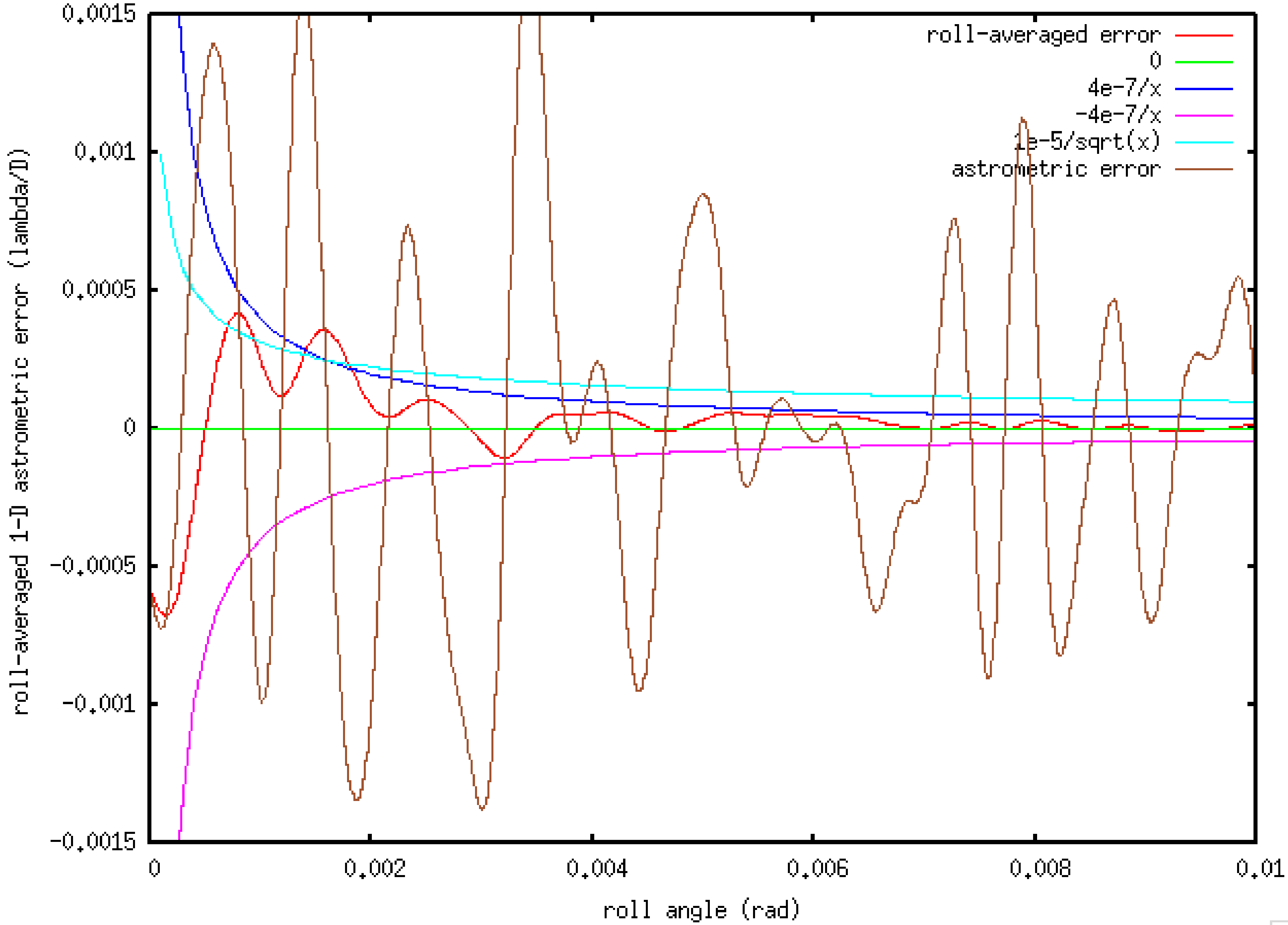

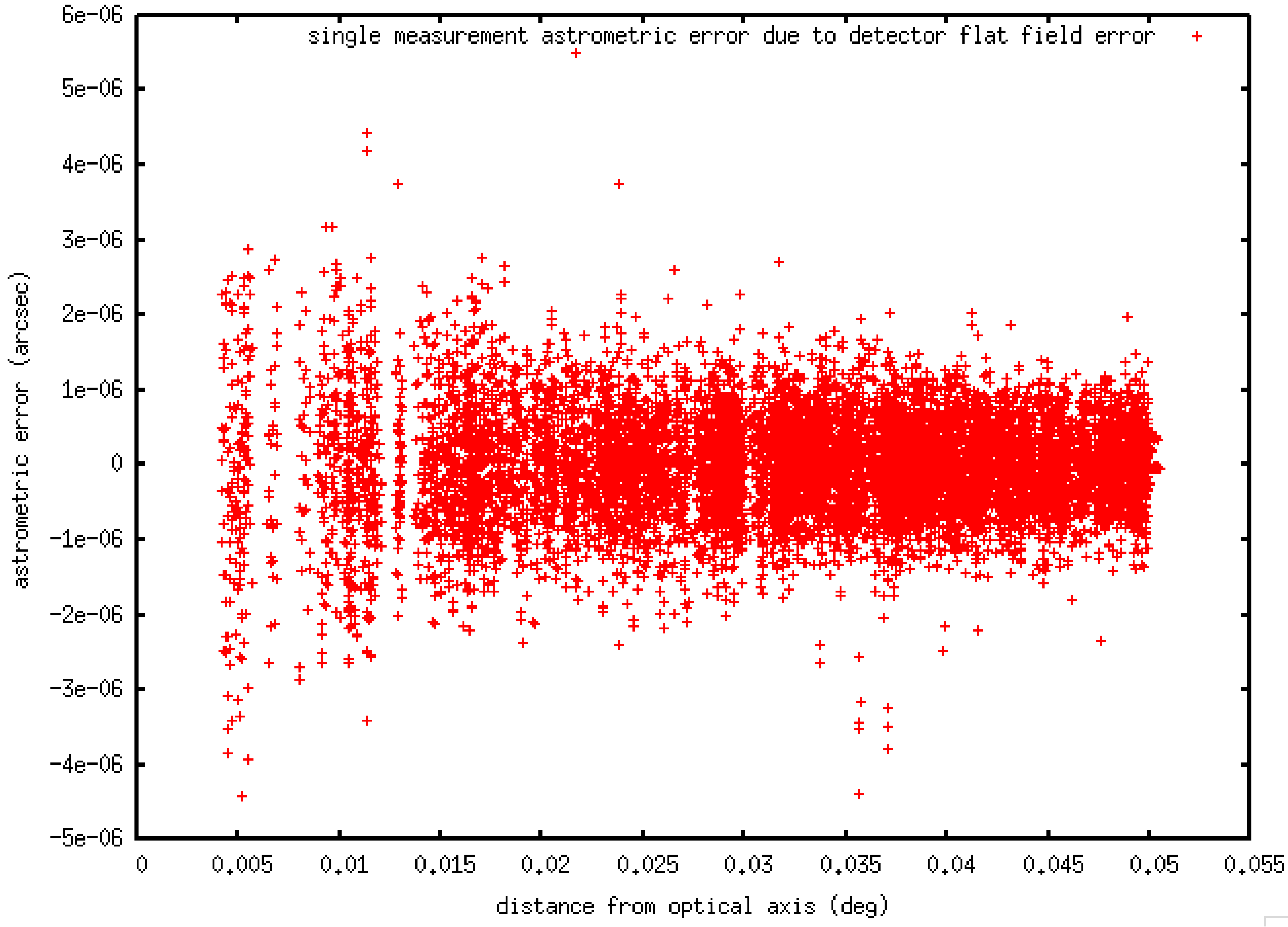

Astrometric error due to flat field errors is ~0.5 uas per star for a 1 rad roll.
Error is stronger for stars closer to the optical axis (less roll averaging)

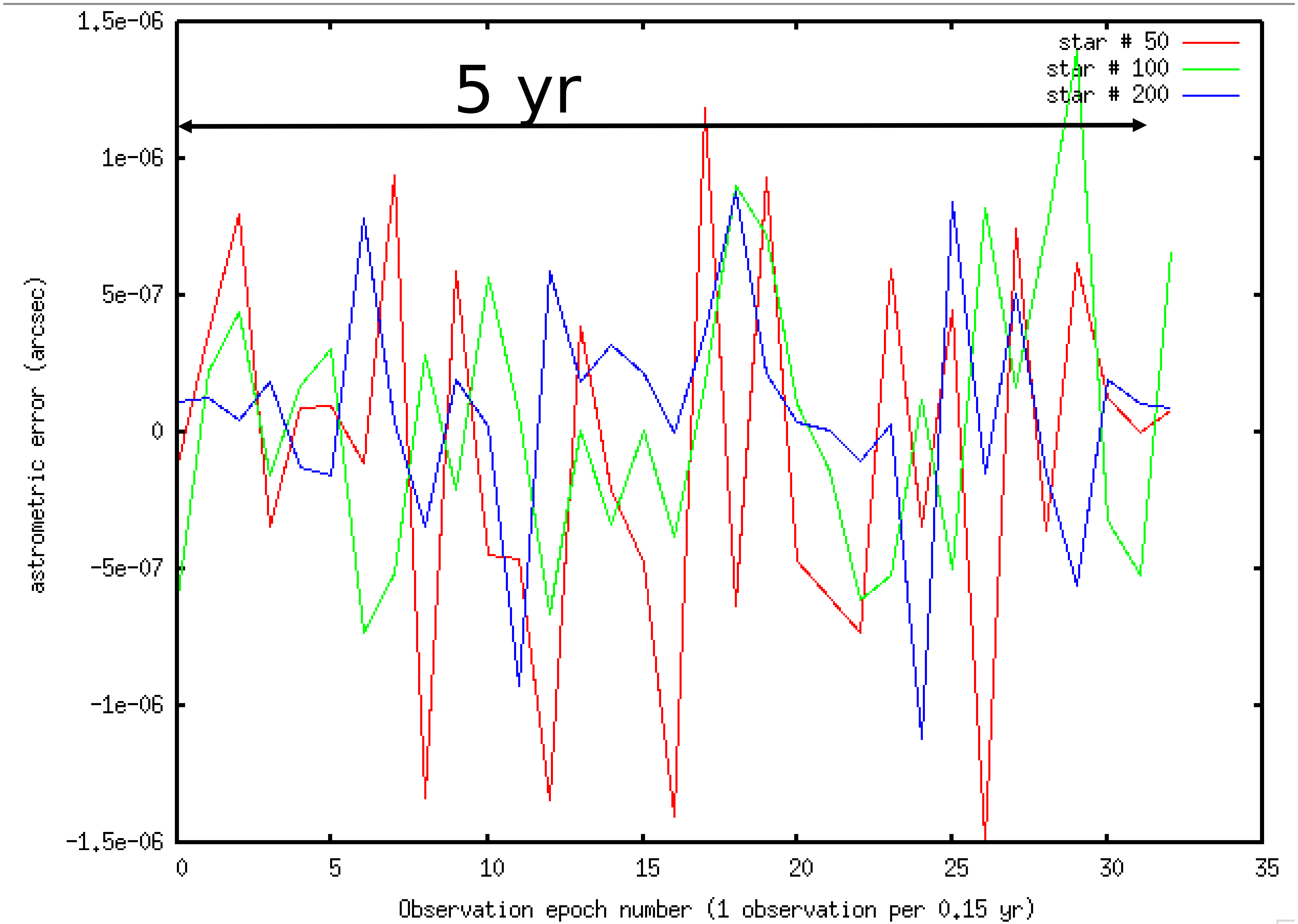

Single star astrometric error due to flat field errors shows no obvious time correlation in this example (1 arcsec / yr proper motion). With smaller proper motion and more distant stars (small parallax), correlation is expected over two timescales : time for proper motion to move star by 1 pixel, and 1 year period due to parallax.

Intra-pixel sensitivity errors are captured in this analysis

Unknown variations of sensitivity within a pixel show the same anti-correlation behavior, and are captured in this analysis.

Example: top half of a pixel less sensitive than bottom half
If PSF is below the pixel, PSF position error is positive
If PSF is above the pixel, PSF position error is negative

A small error in sensitivity between pixels is similar to a larger error within a pixel.

Intra-pixel sensitivity errors can be simulated by the same analysis as shown here, but with a finer sampling.

Dynamic distortions

Definition: Any change between observations epochs

These changes introduce errors in the measured position of background stars or on the distortion change measured by the spikes image.

Description of main error terms:

- Variation in the optical shape of mirrors M2 and M3 due to thermal and mechanical stresses introduces astrometric distortions that change between the observation epochs
- Rigid body motion of optics (telescope alignment)
- Focal plane array geometry: motion and distortion of individual detector chip due to temperature fluctuation and mechanical stress
- Variations in the flat field response of the detector

Impact and mitigation:

Low order components of dynamic errors are calibrated by the diffraction spikes. To measure how distortions change between observations, the motion of the spikes is measured by comparison of the spike images between the different observation epochs.

Errors in this estimate come from

- photon noise (spikes, zodi)
- changes in the pixel response between the 2 epochs
- interpolation between spikes (no signal between spikes)

Time-variable distortions are not perfectly estimated by the spikes -> astrometric error

Numerical simulation approach

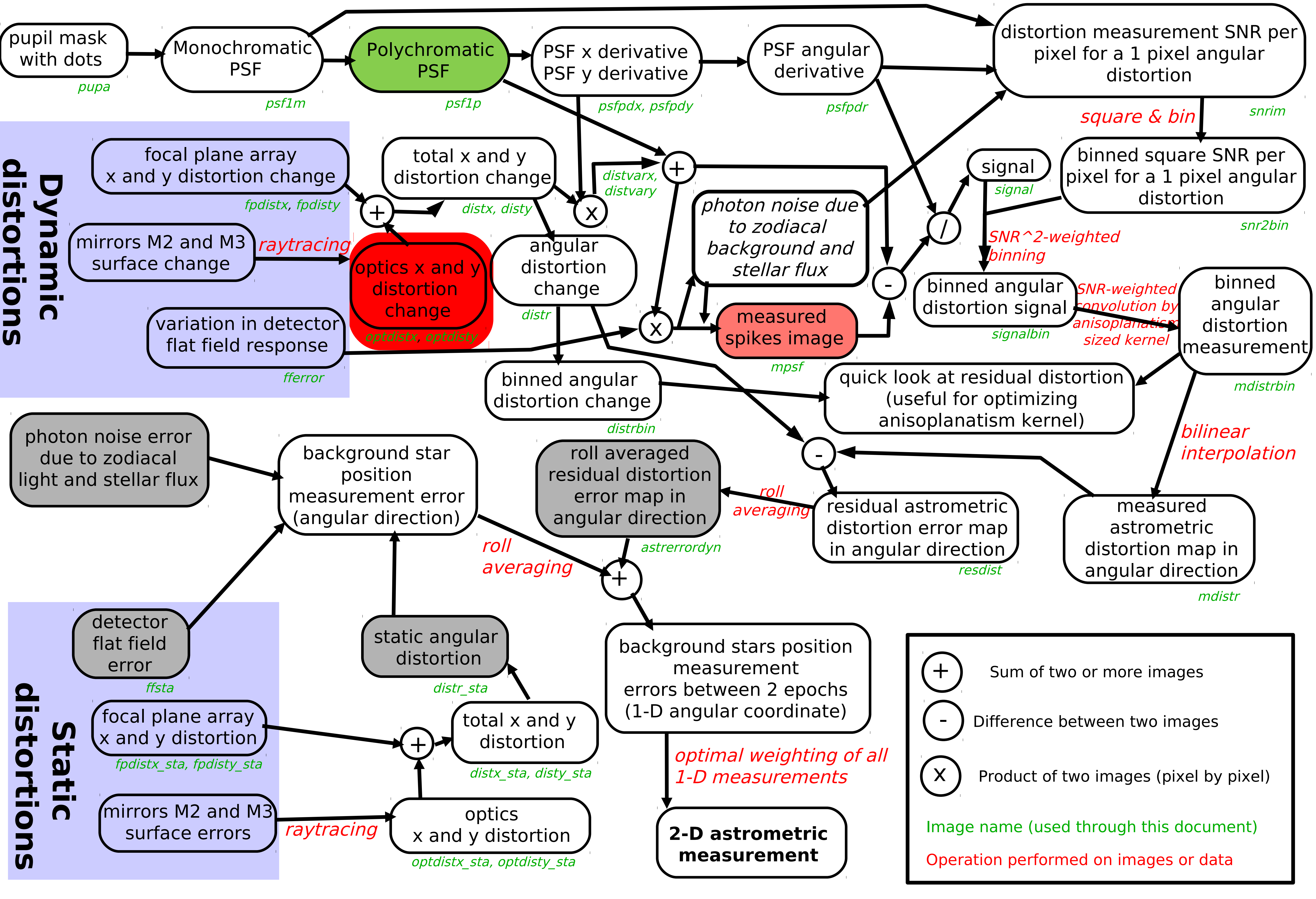

Time-variable distortions: M2 and M3

Thermal variations in substrate + mirror mounting:
On 150-350mm apertures, better than 0.1nm RMS wavefront insertion repeatability with 0.25 C temperature stability. (Jay Daniel, L-3 Tinsley, private communication)
Assuming 100mK temperature stability-> 40 pm RMS stability
Material creep :
probably slow process (timescale > single observation) which can be tracked during course of mission by averaging distortions over several consecutive observations. -> not included

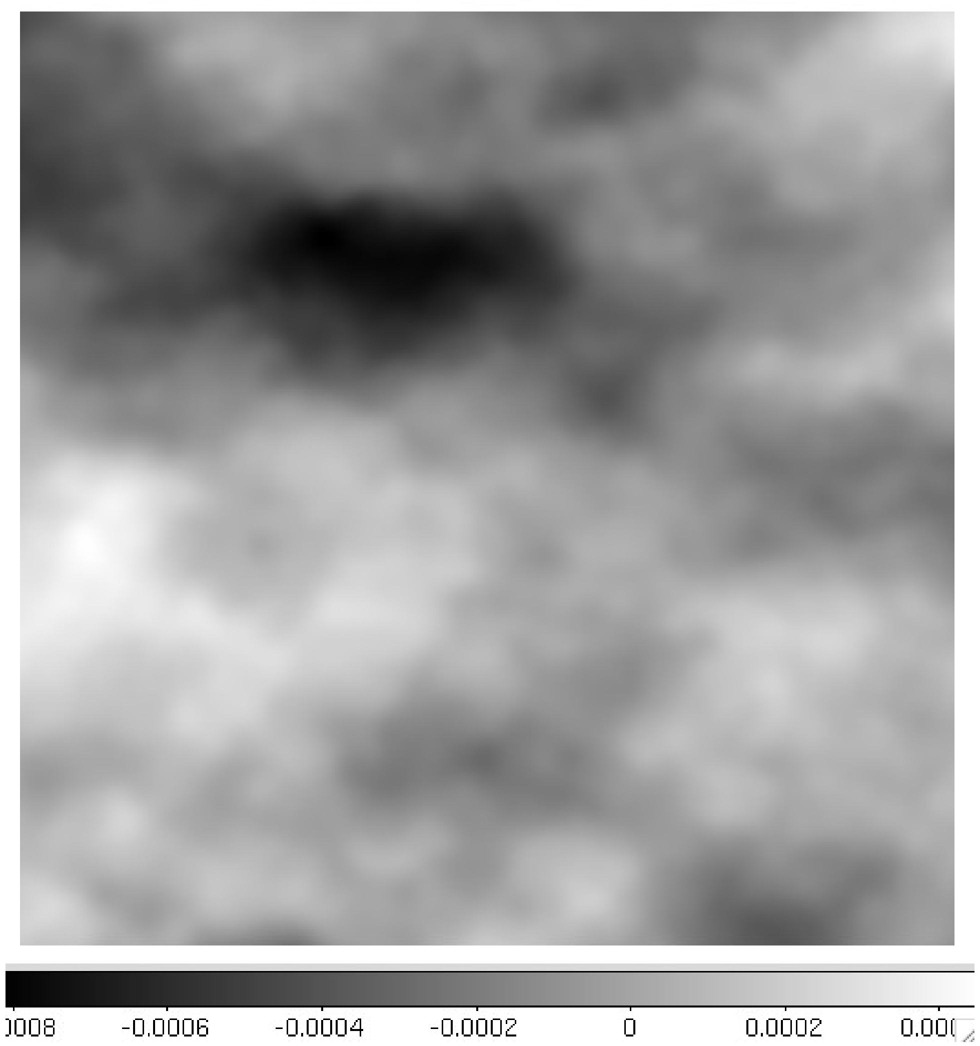

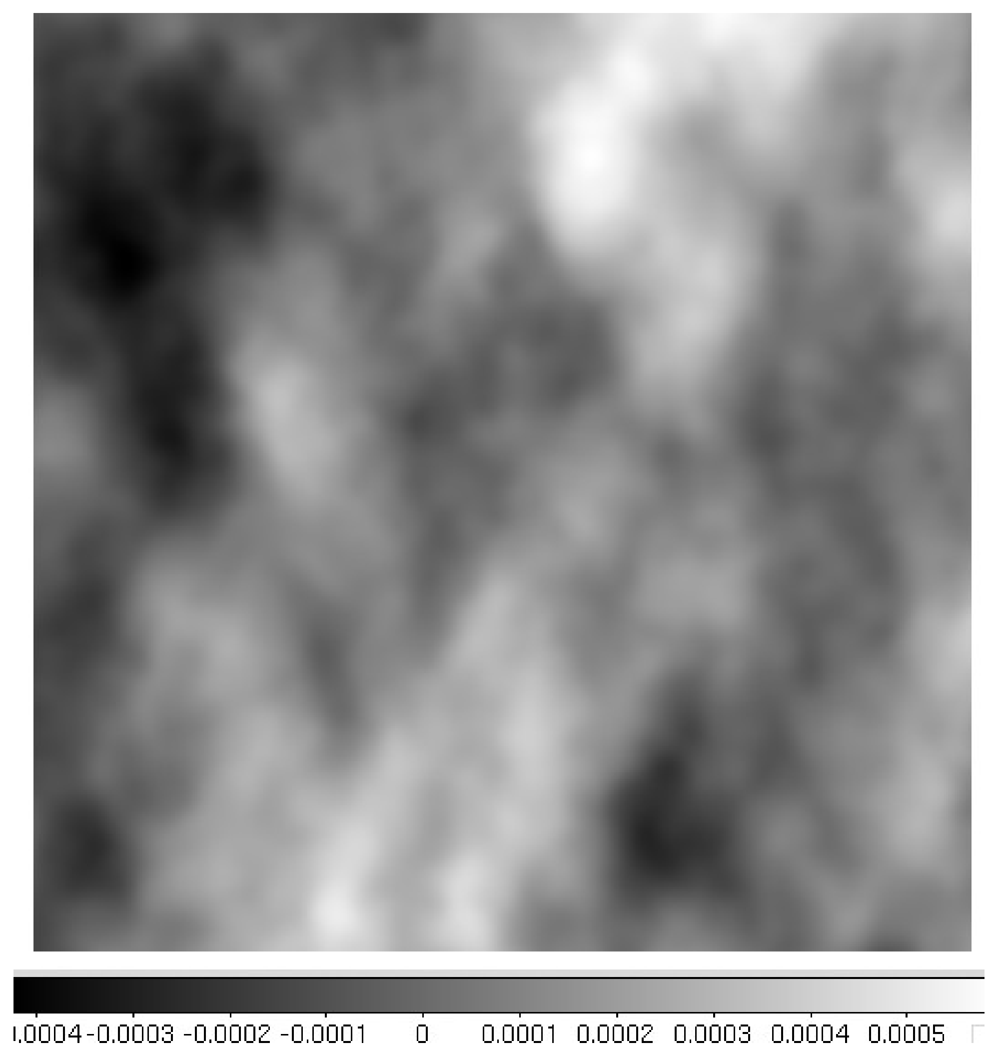

x and y astrometric distortions due to change in the shape of optics is shown on the left.

Same as static optical distortions, but scaled by 3%. Unit = pixel (44 mas)

Numerical simulation approach

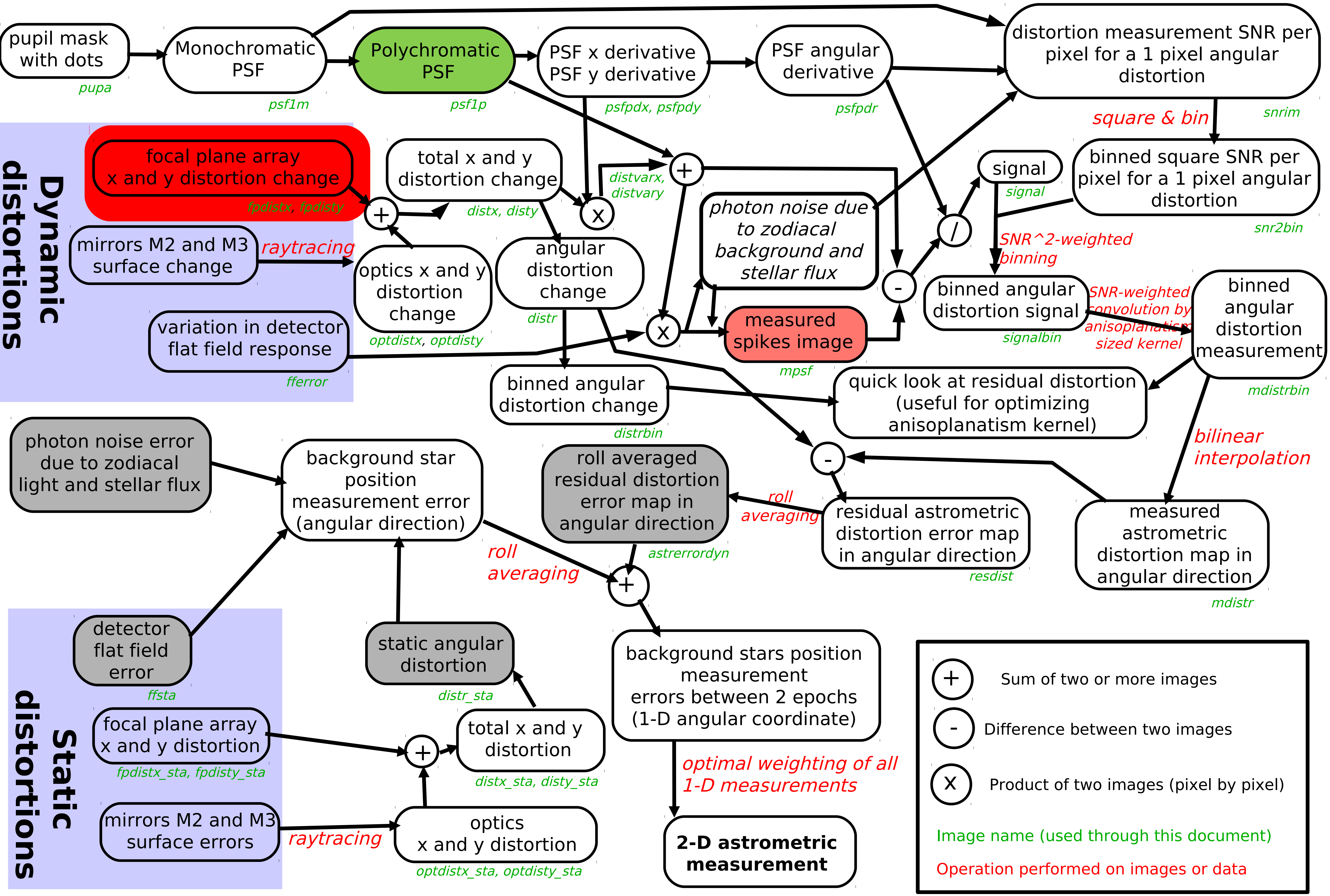

Detector array distortions

A 100 mK temperature change on a 4k detector changes its linear size by 0.00172 pixel, assuming Si (CTE=4.2e-6). This is simulated by a low order term in x distortion with +/- 1e-3 pixel and period ~ single 4k detector size.Translation between detector chips not included here - would need to be fitted as a translation for each chip.

Unit = pixel (44 mas)

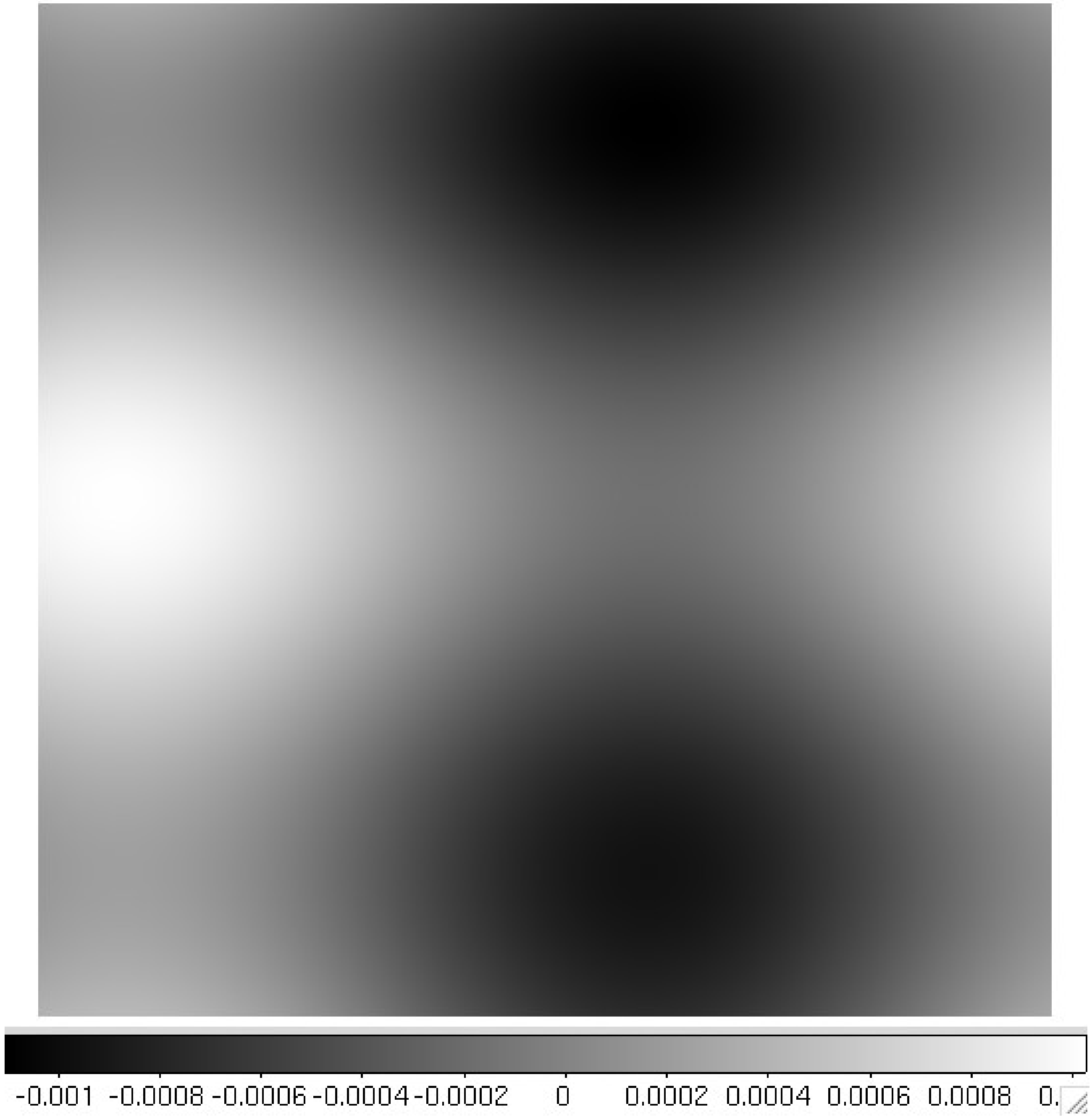

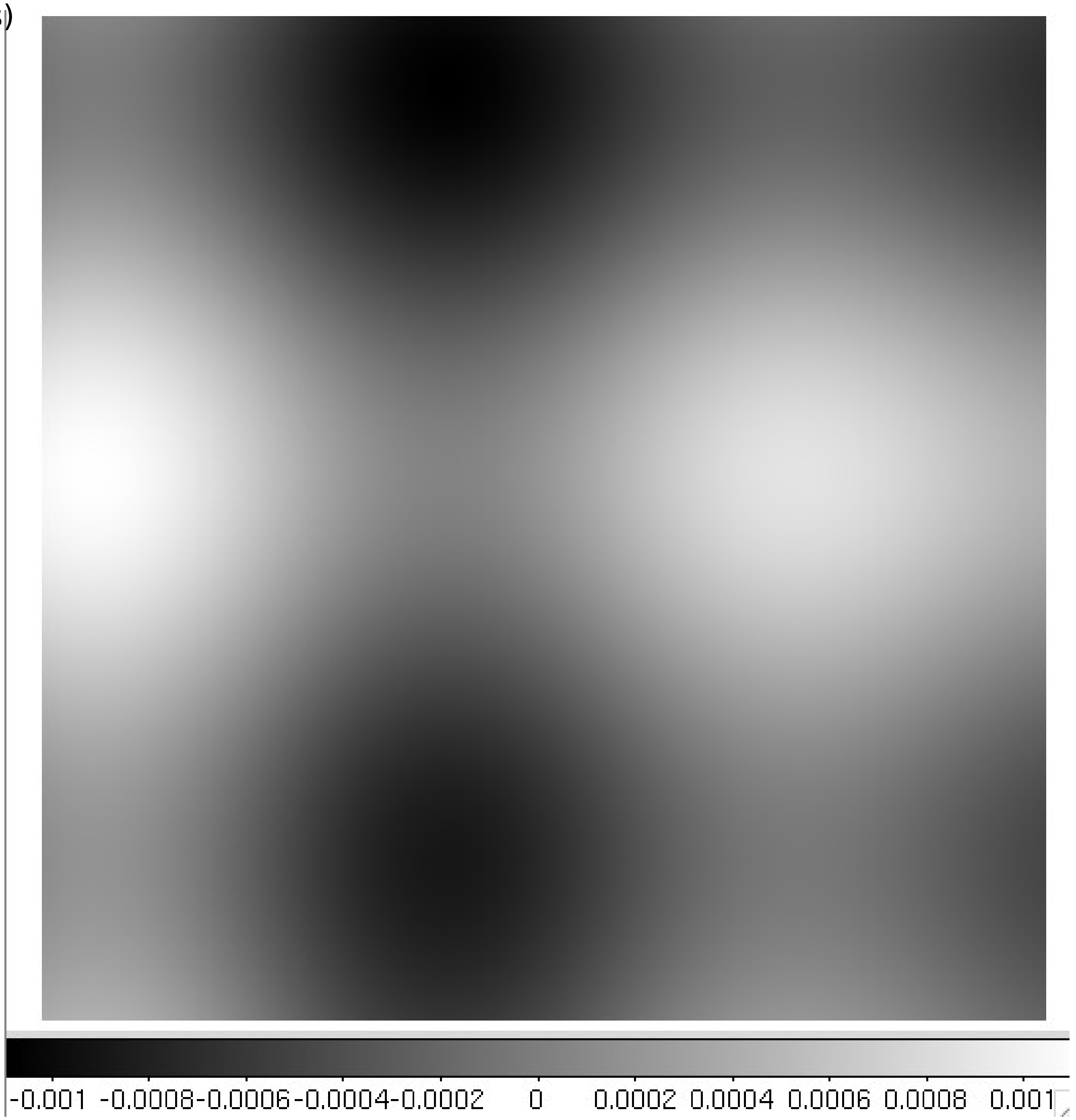

Numerical simulation approach

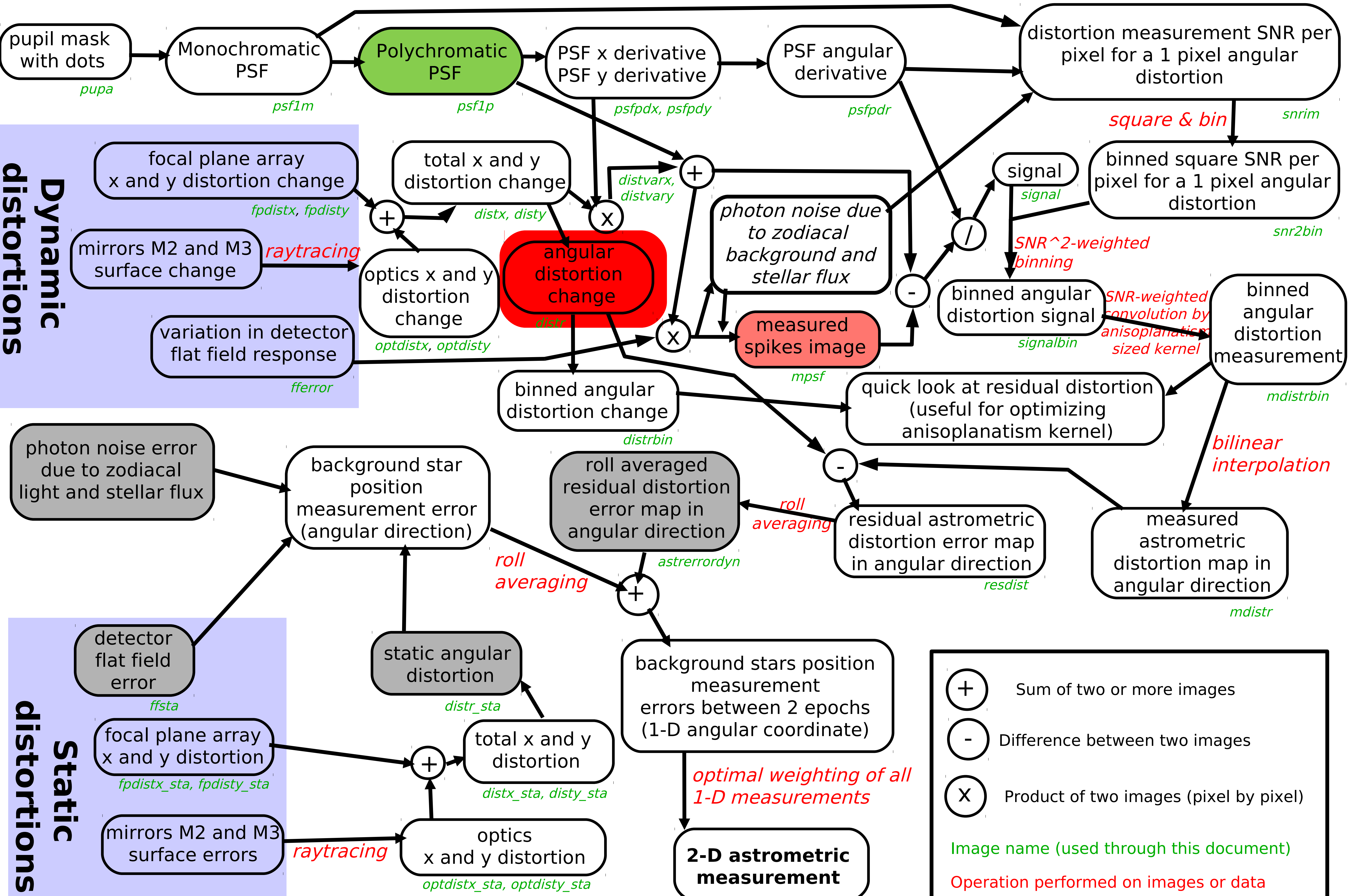

Total angular distortion change

Unit = pixel (44 mas)
Amplitude ~ 1/1000 pixel (44 uas)

Flat field change between epochs

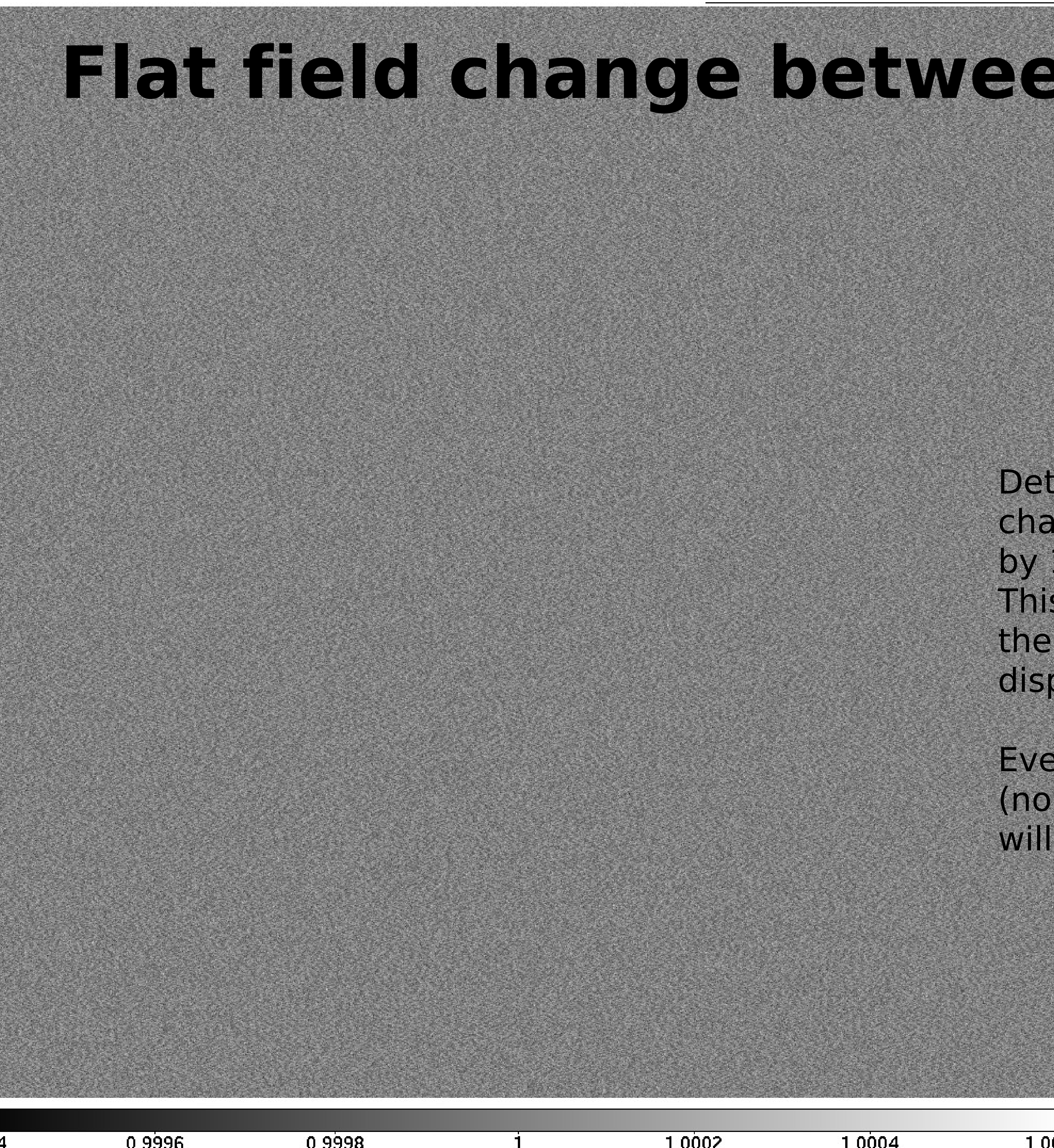

Detector response map changes between observation by 1e-4 (RMS)
This will produce an error in the measurement of spikes displacements.

Even if the spikes are steady (no distortion), a distortion will be measured.

Numerical simulation approach

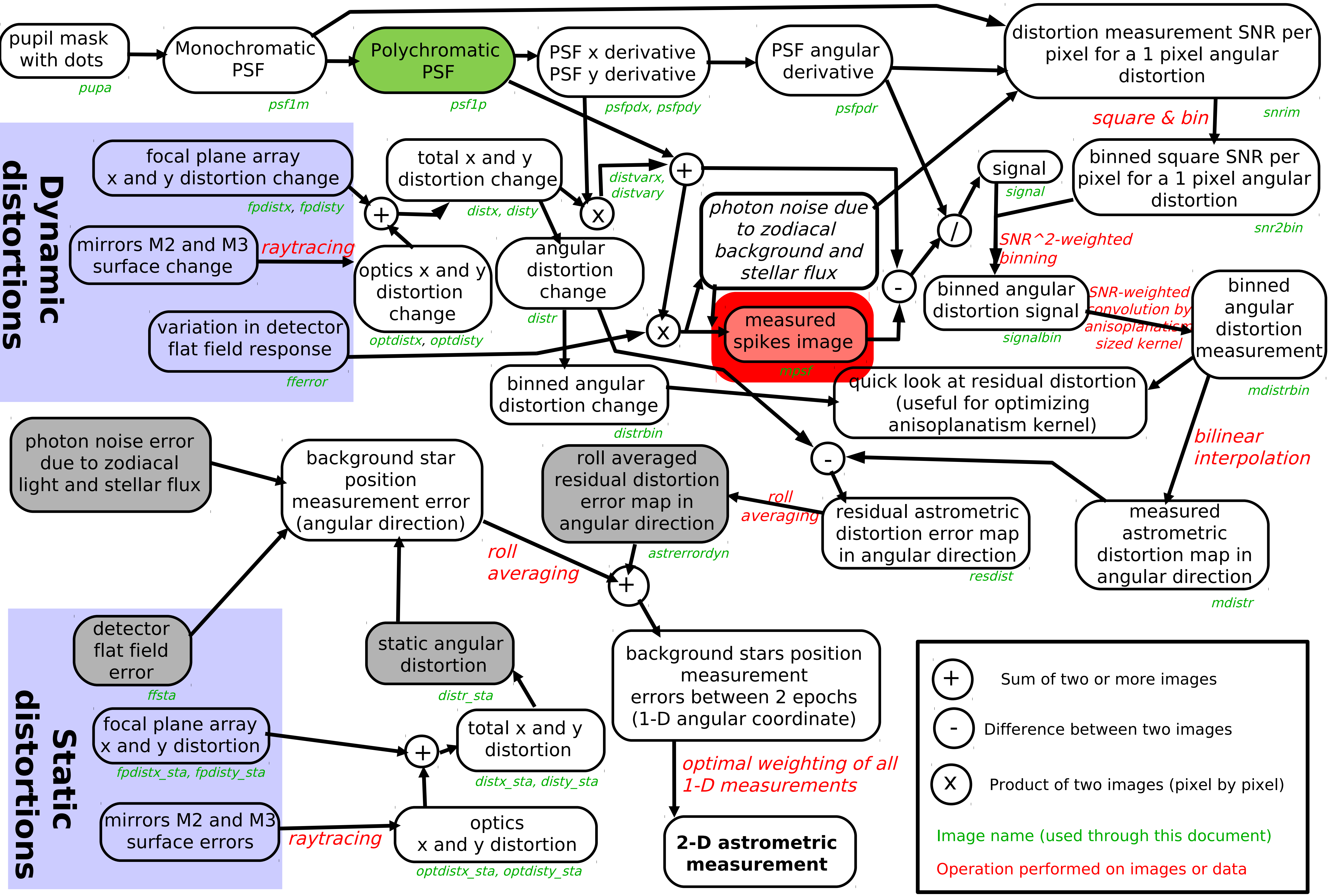

Spikes image, 0.2 deg FOV

Spike image is computed by:

step 1: compute derivative in x and y for the spikes

step 2: multiply derivative by x and y distortion maps

step 3: add noise terms (photon noise, readout noise, flat field noise)

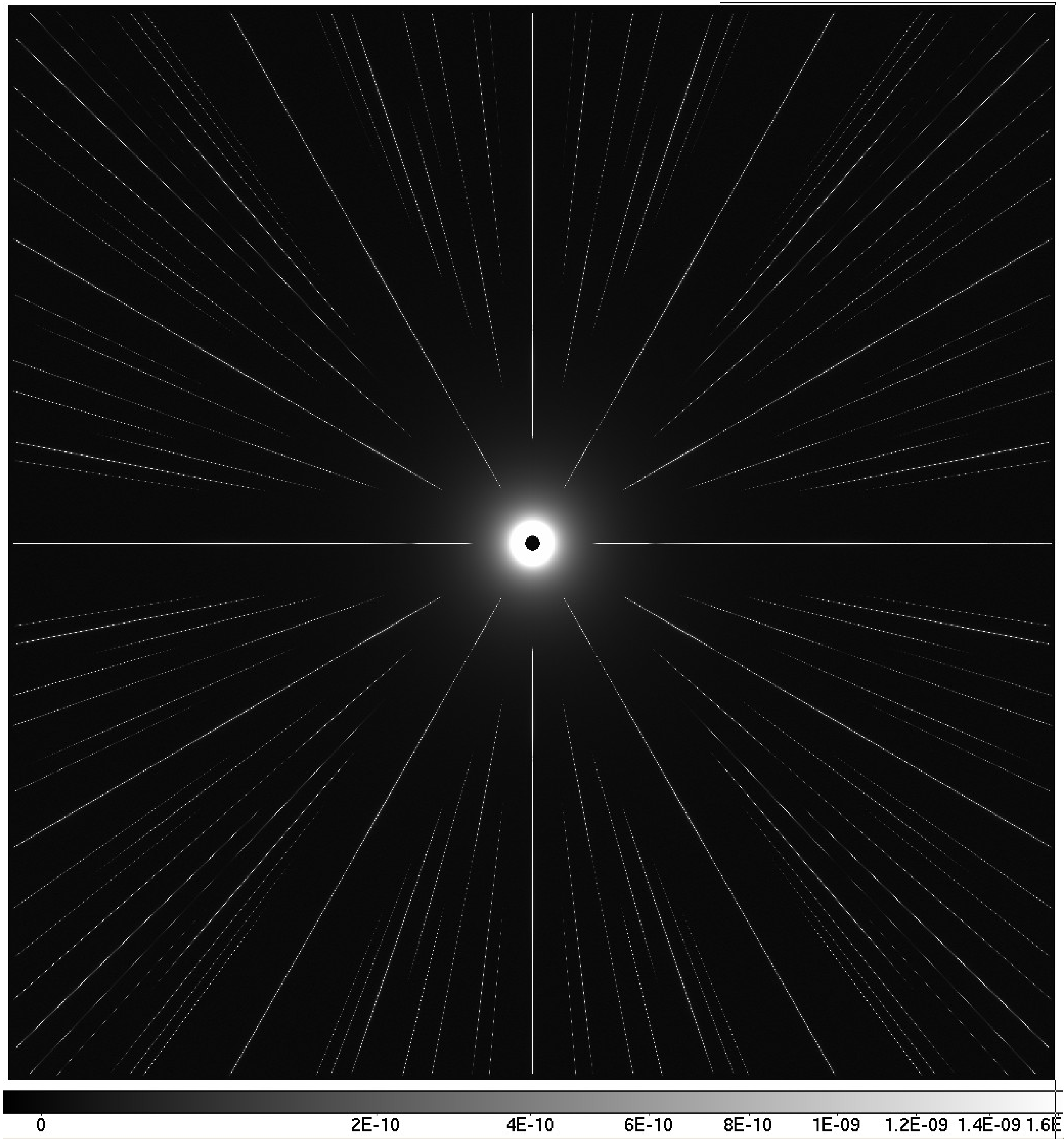

Spikes image (central region, 3'x3')

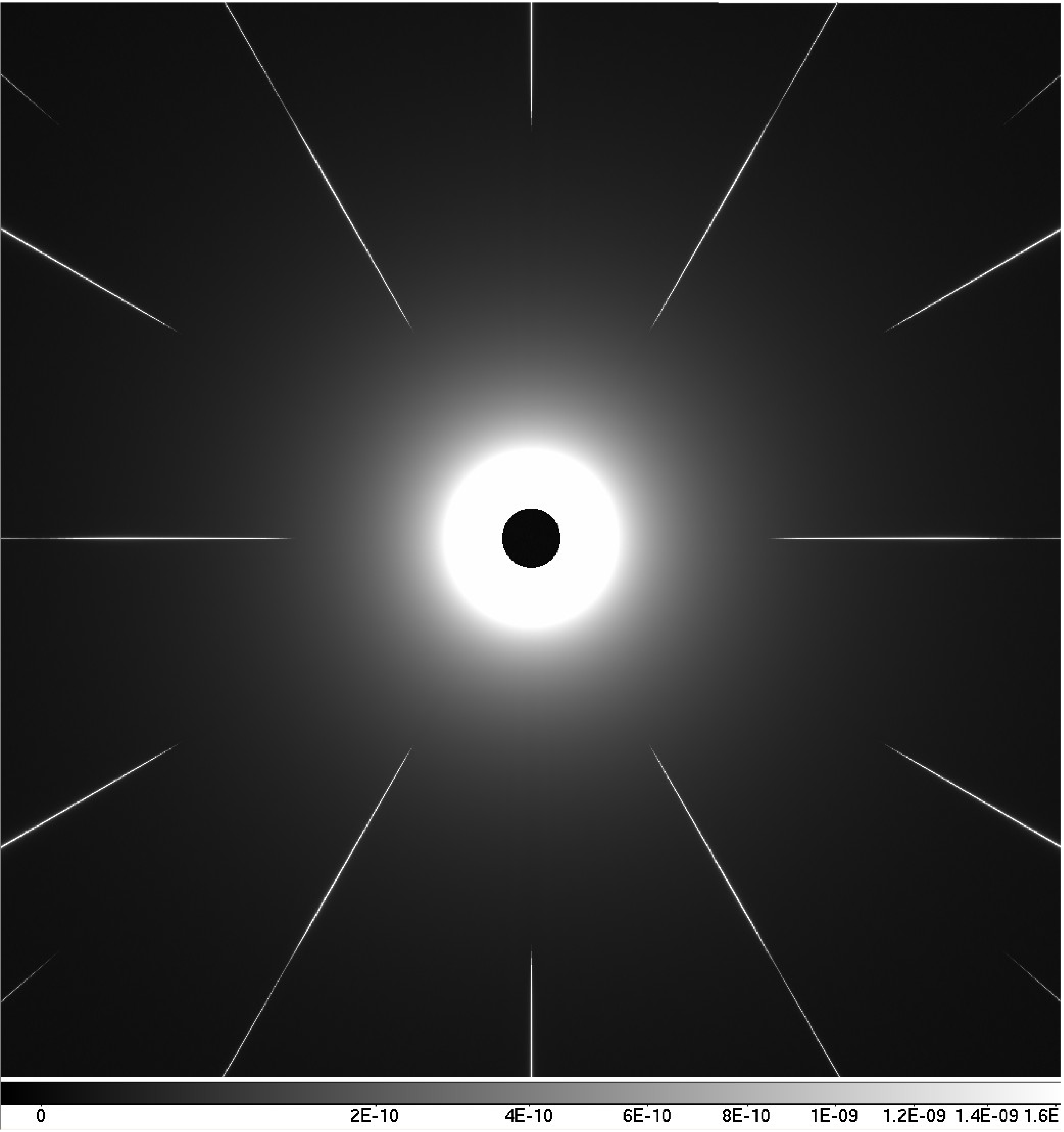

Central part of the field is blocked by the coronagraph pickup mirror.

The spikes do not extend inward to the coronagraphic field.

Zodi-subtracted spikes image, no background stars

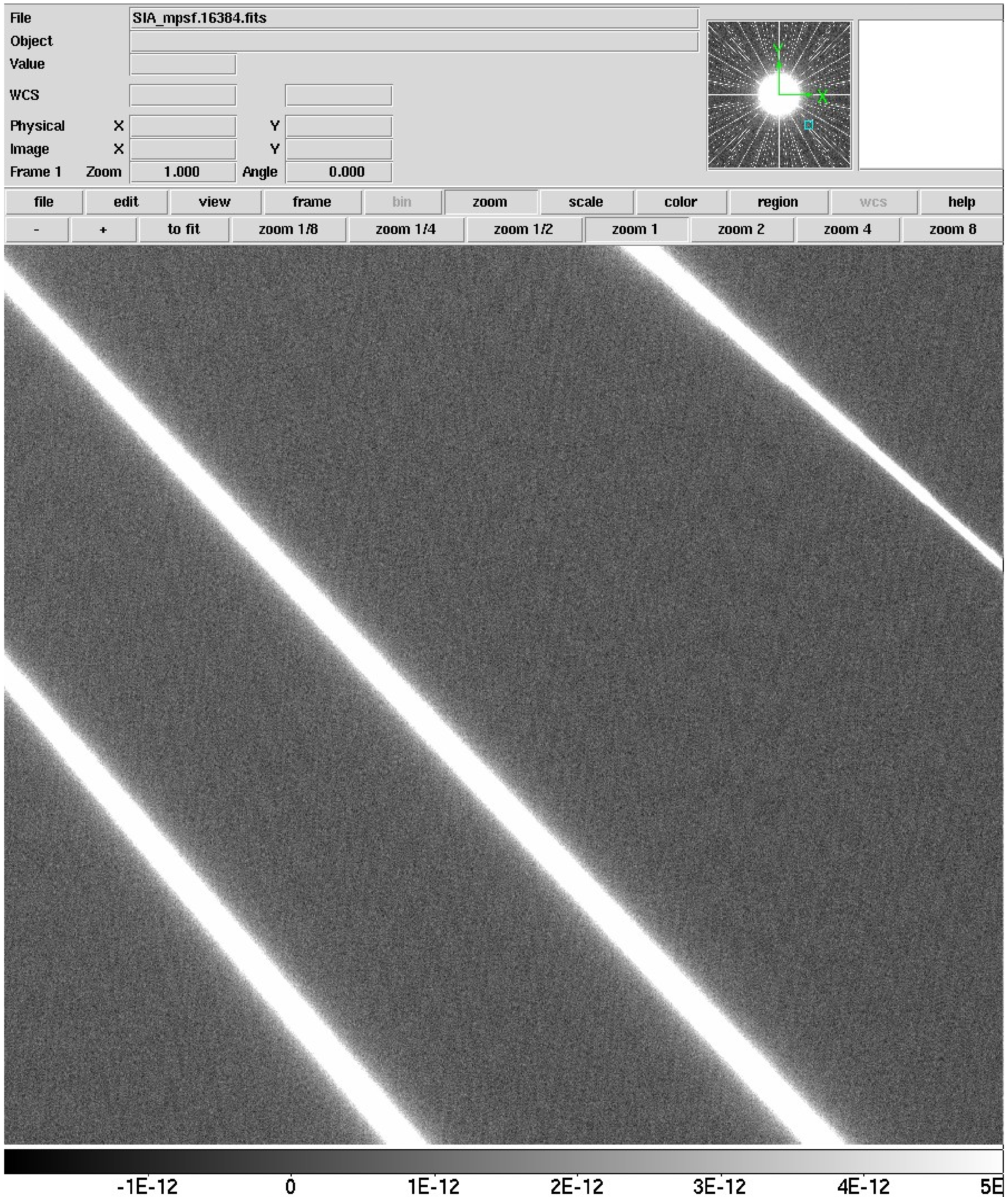

Photon noise from spikes and zodiacal light are visible in this frame.

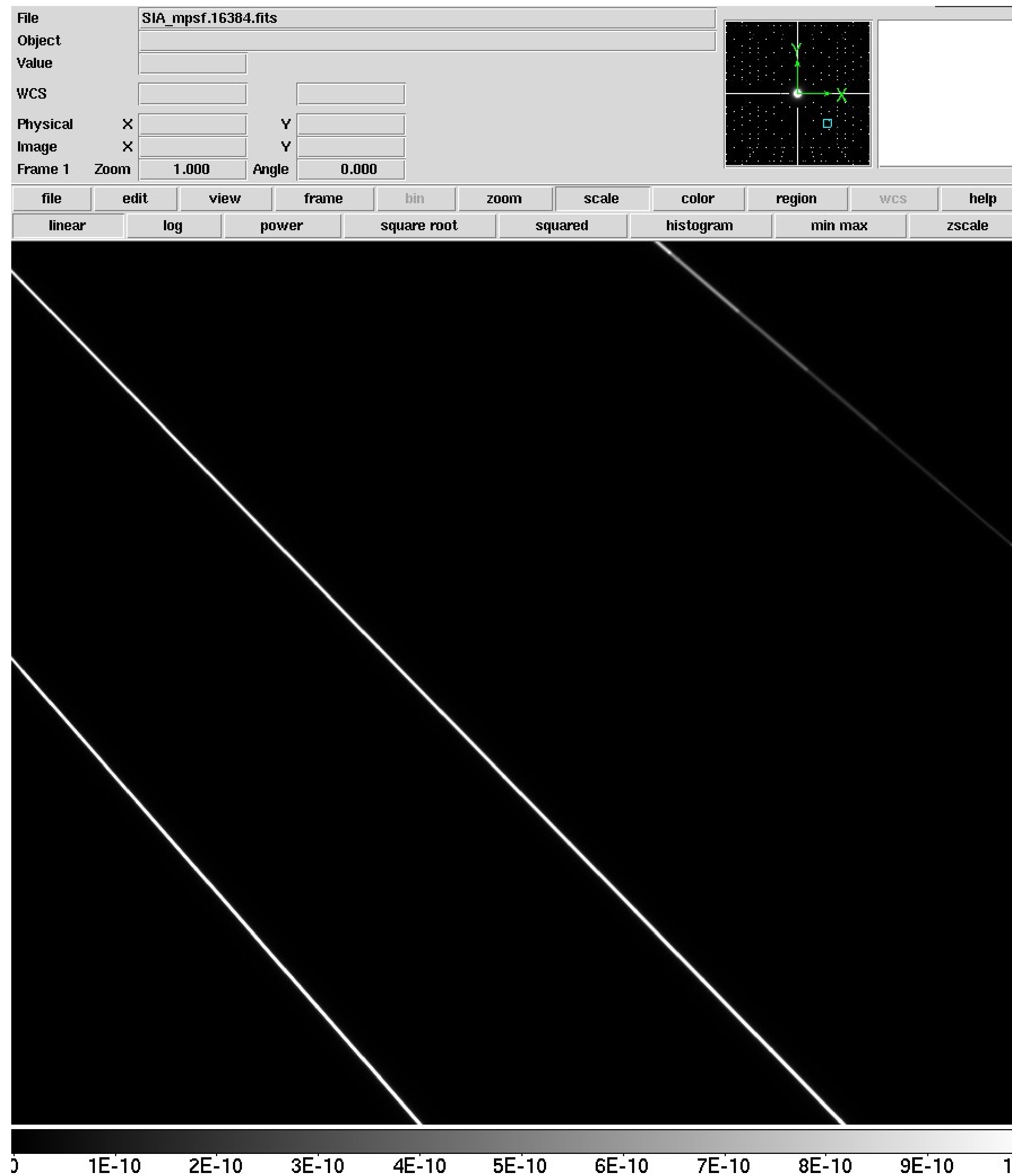

Spikes are l/D wide

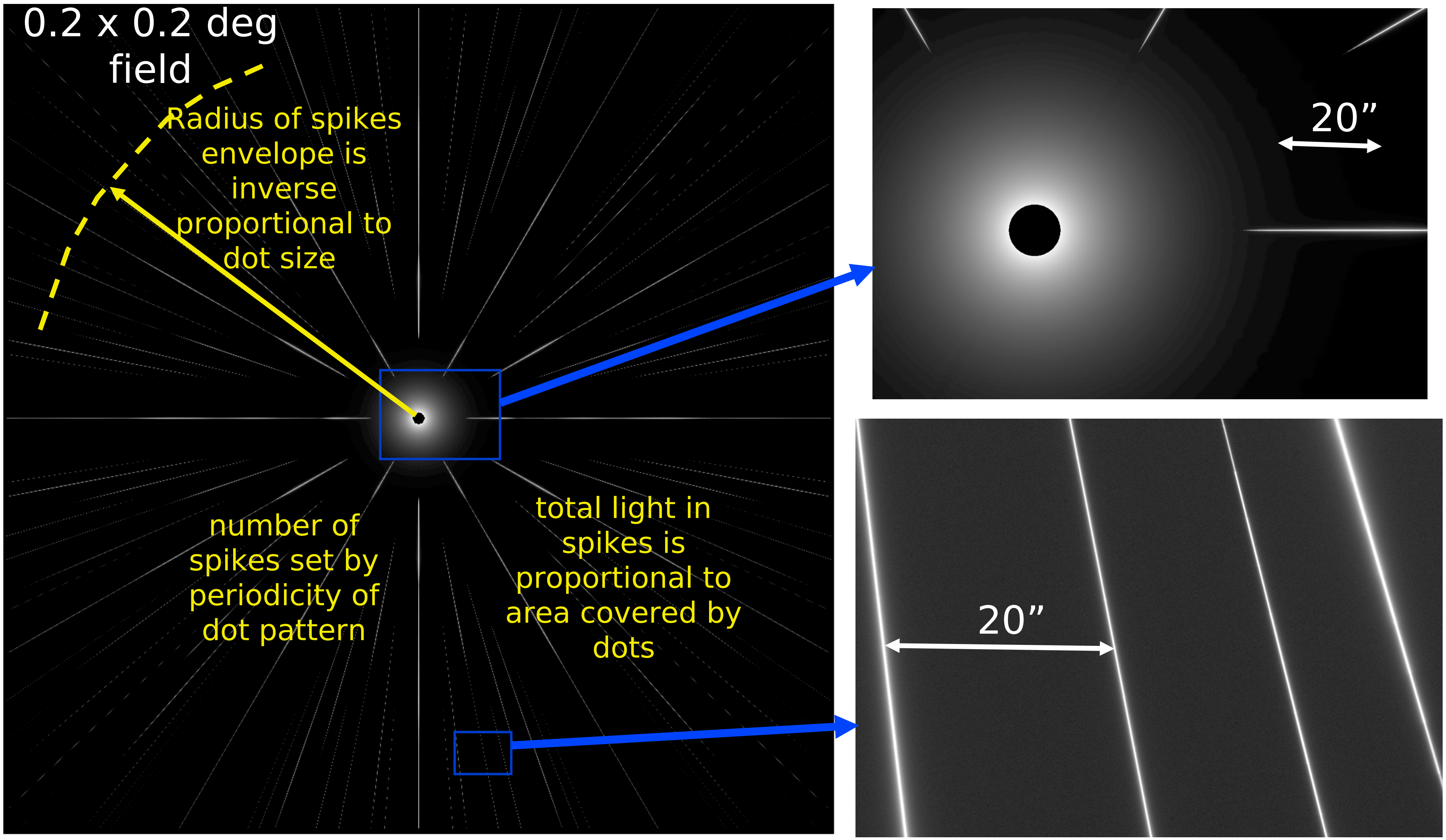

The overall size of the spike envelope, the spikes density (spacing between spikes) and brightness can be chosen by design of the dot pattern.

Numerical simulation approach

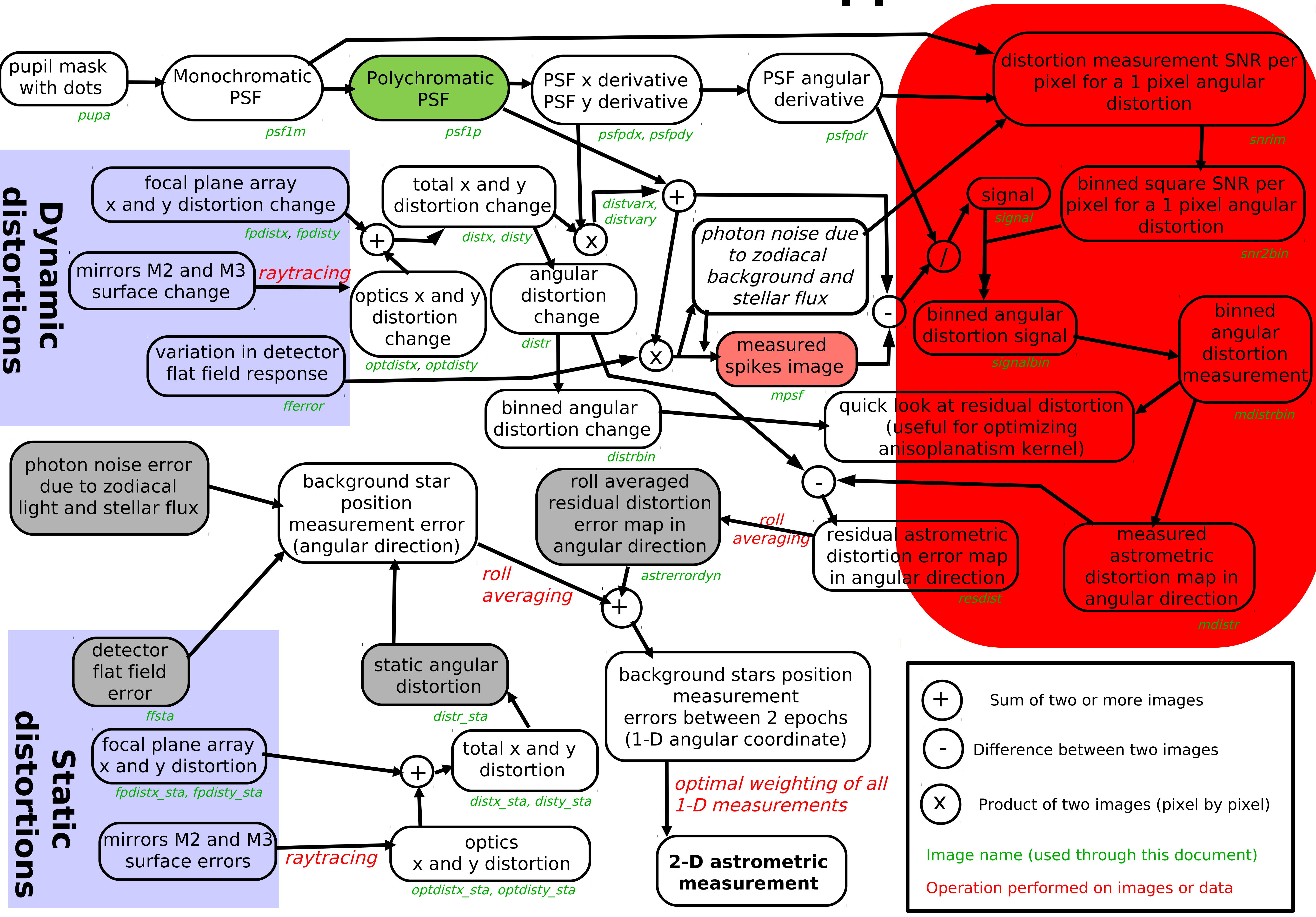

Distortion measurement

Compute SNR for a 1 pixel angular distortion for each pixel -> SNRmap
Compute signal (unit = pixel of angular distortion) for each pixel = difference between ideal spike image and measured spike image, divided by dImage/dDistortion -> Signalmap

To speed up computation, Signalmap and SNRmap are binned to lower resolution (with optimal weights derived from SNRmap)

Numerical simulation approach

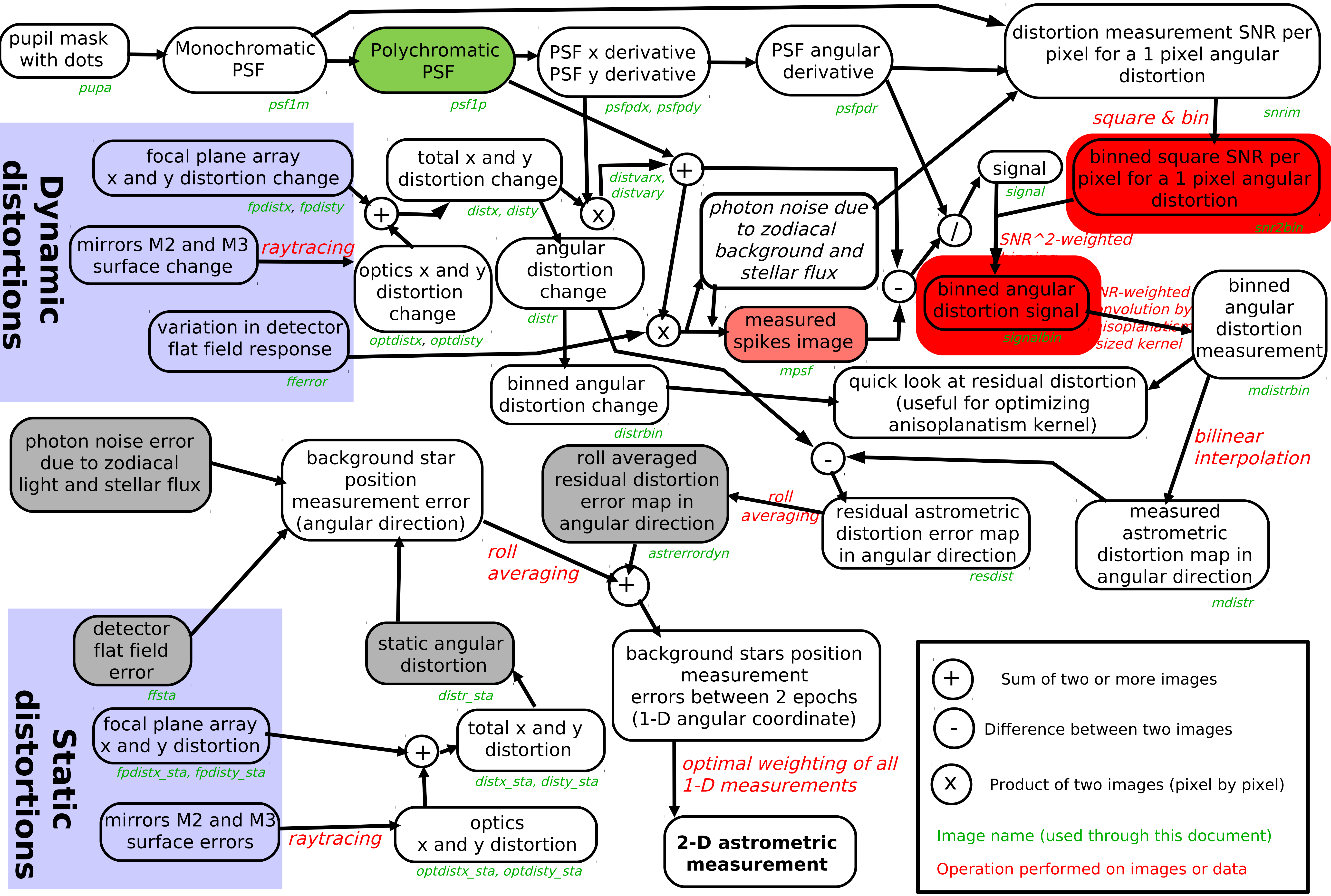

Distortion measurement

SNR^2

binned Signal (using SNR^2 weighting within each bin)
Value set to zero where SNR is below threshold

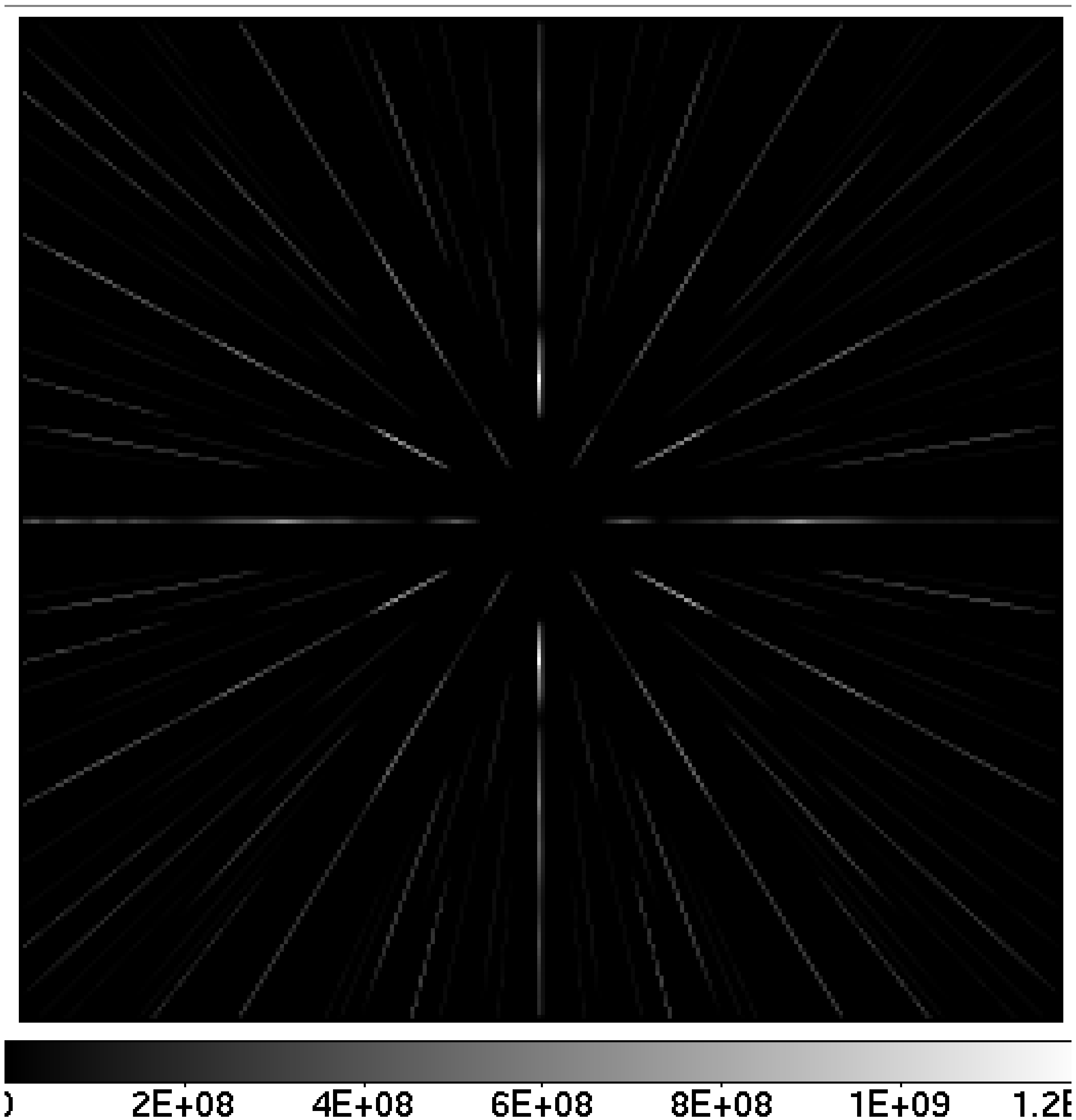

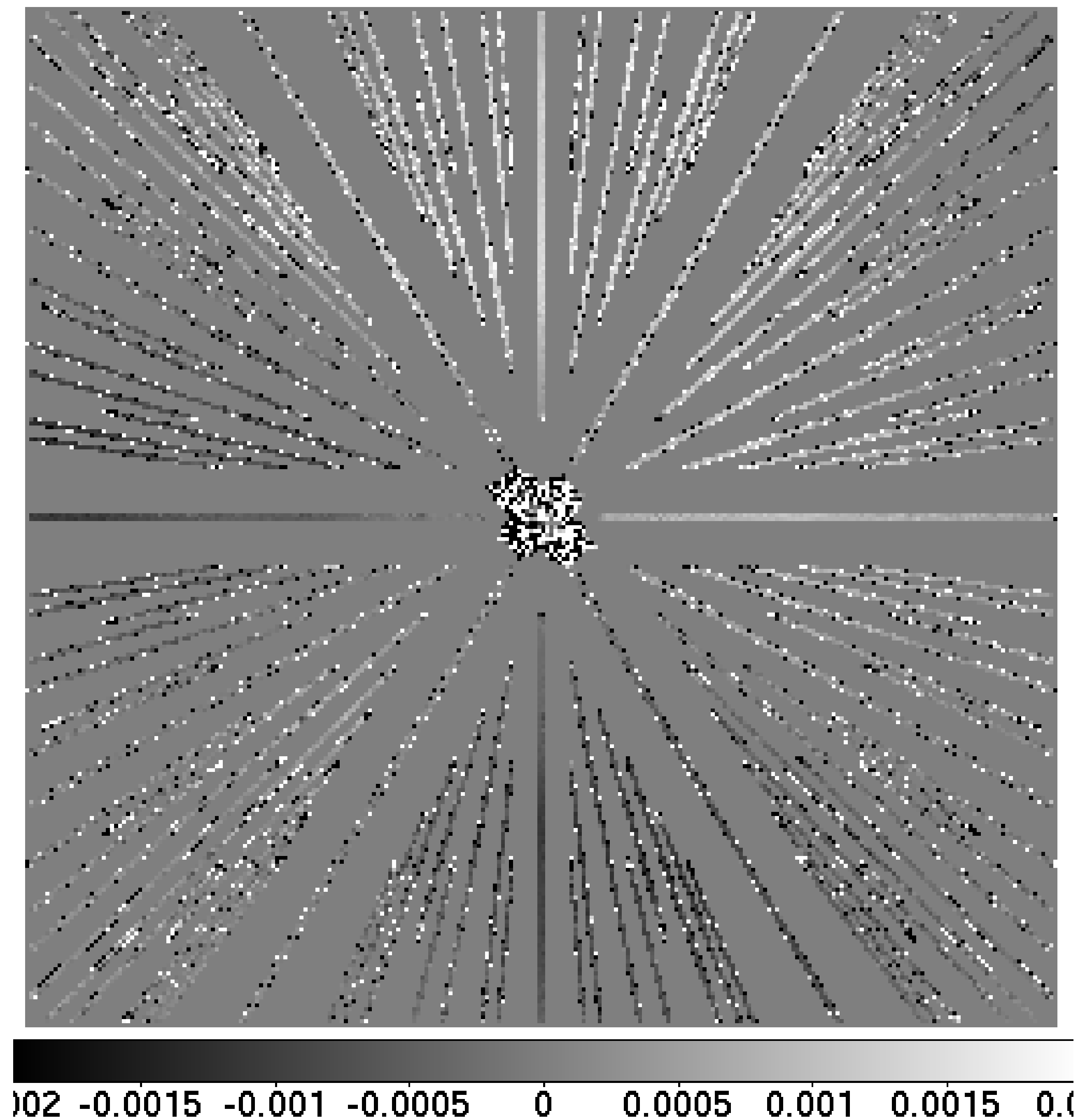

Numerical simulation approach

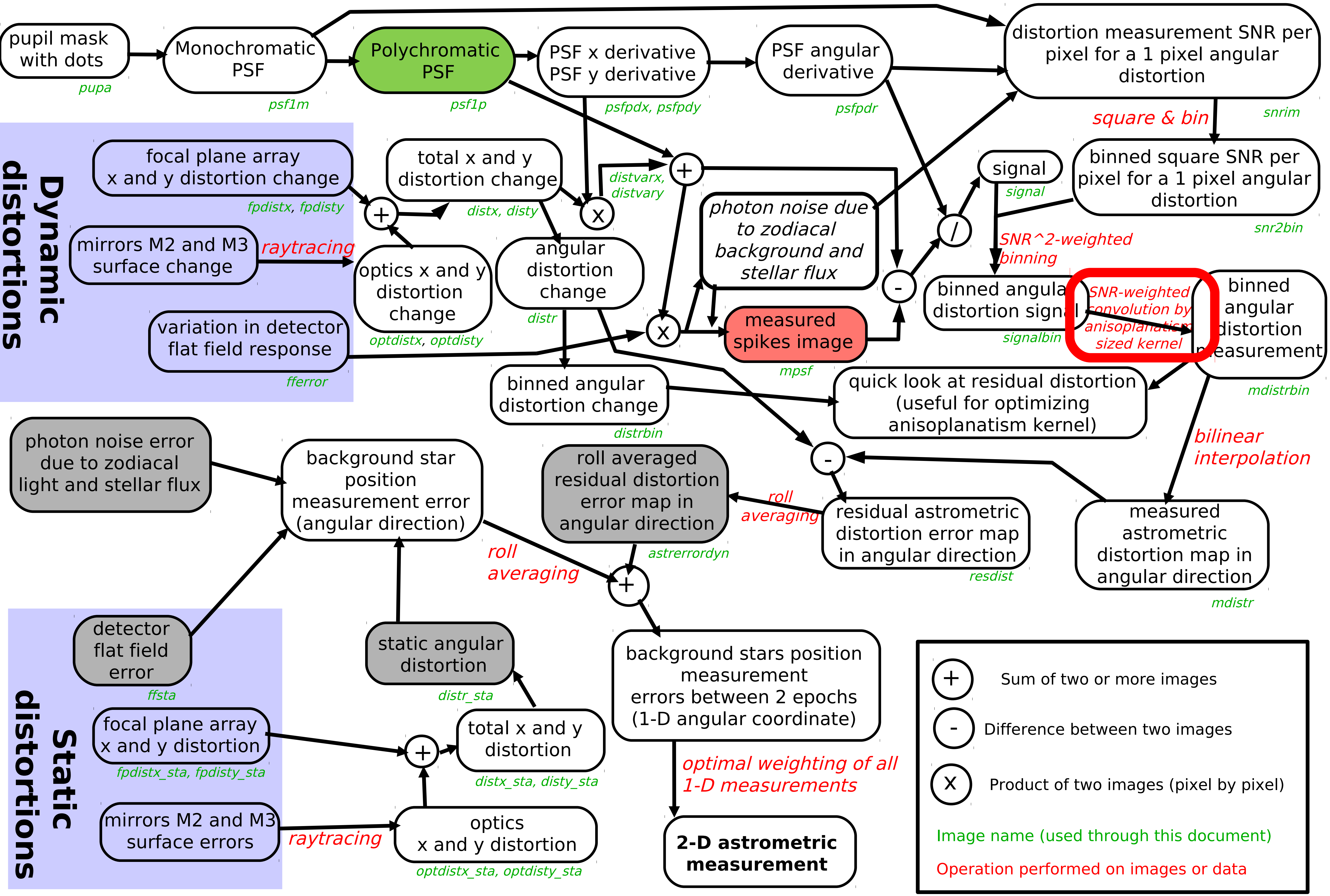

Distortion interpolation

Convolve signal x SNR^2 by gaussian kernel, with sigma of the kernel ~ anisoplanatism patch size

Problem: next to a bright spike, the solution will give a flat value with a sharp jump when moving to the next spike.
Estimate for each pixel the effective centroid of the result (different from the pixel location), and the local slope of the distortion -> using these 2 quantities, correct for the centroid offset error.

Distortion interpolation

```
for(ii=0;ii<sizeb*sizeb;ii++)
  distarray[ii] = 0.0;

for(ii0=0;ii0<sizeb;ii0++)
  for(jj0=0;jj0<sizeb;jj0++)
    {
      v = 0.0;
      vx = 0.0;
      vy = 0.0;
      xt = 0.0;
      yt = 0.0;
      vcnt = 0.0;
      vxcnt = 0.0;
      vycnt = 0.0;

      for(kk=0;kk<NBpt;kk++)
        {
          ii = iiarray[kk]-ii0;
          jj = jjarray[kk]-jj0;
          x = 1.0*ii*SIA_pixscale*binfact; // radian
          y = 1.0*jj*SIA_pixscale*binfact; // radian
          r2 = x*x+y*y;
          r2 /= SIA_corr_aniso_rad*SIA_corr_aniso_rad;
          if(r2<9.0)
            {
              v += varray[kk]*snr2array[kk]*exp(-r2);
              xt += x*snr2array[kk]*exp(-r2);
              yt += y*snr2array[kk]*exp(-r2);
              vcnt += snr2array[kk]*exp(-r2);
            }
        }
      if(vcnt > eps)
        {
          v /= vcnt;
          xt /= vcnt; // effective x
          yt /= vcnt; // effective y
        }

      for(kk=0;kk<NBpt;kk++)
        {
          ii = iiarray[kk]-ii0;
          jj = jjarray[kk]-jj0;
          x = 1.0*ii*SIA_pixscale*binfact; // radian
          y = 1.0*jj*SIA_pixscale*binfact; // radian
          r2 = x*x+y*y;
          r2 /= SIA_corr_aniso_rad*SIA_corr_aniso_rad;
          if(r2<9.0)
            {
              vx += (varray[kk]-v)*snr2array[kk]*(x-xt)*exp(-r2);
              vy += (varray[kk]-v)*snr2array[kk]*(y-yt)*exp(-r2);
              vxcnt += snr2array[kk]*(x-xt)*(x-xt)*exp(-r2);
              vycnt += snr2array[kk]*(y-yt)*(y-yt)*exp(-r2);
            }
        }
      if(vxcnt>eps)
        vx /= vxcnt;
      if(vycnt>eps)
        vy /= vycnt;

      v -= xt*vx;
      v -= yt*vy;
      distarray[jj0*sizeb+ii0] = v;
    }
```

kk is an index to the list of high SNR measurements (5% best pixels)

Convolution by kernel

This is the effective centroid to whic the computed value corresponds. Th centroid gets pulled to bright spikes.

Compute local 2D derivative of the measured distortion

Compensation of error due to centroid offset and local 2D derivative of distortion

Numerical simulation approach

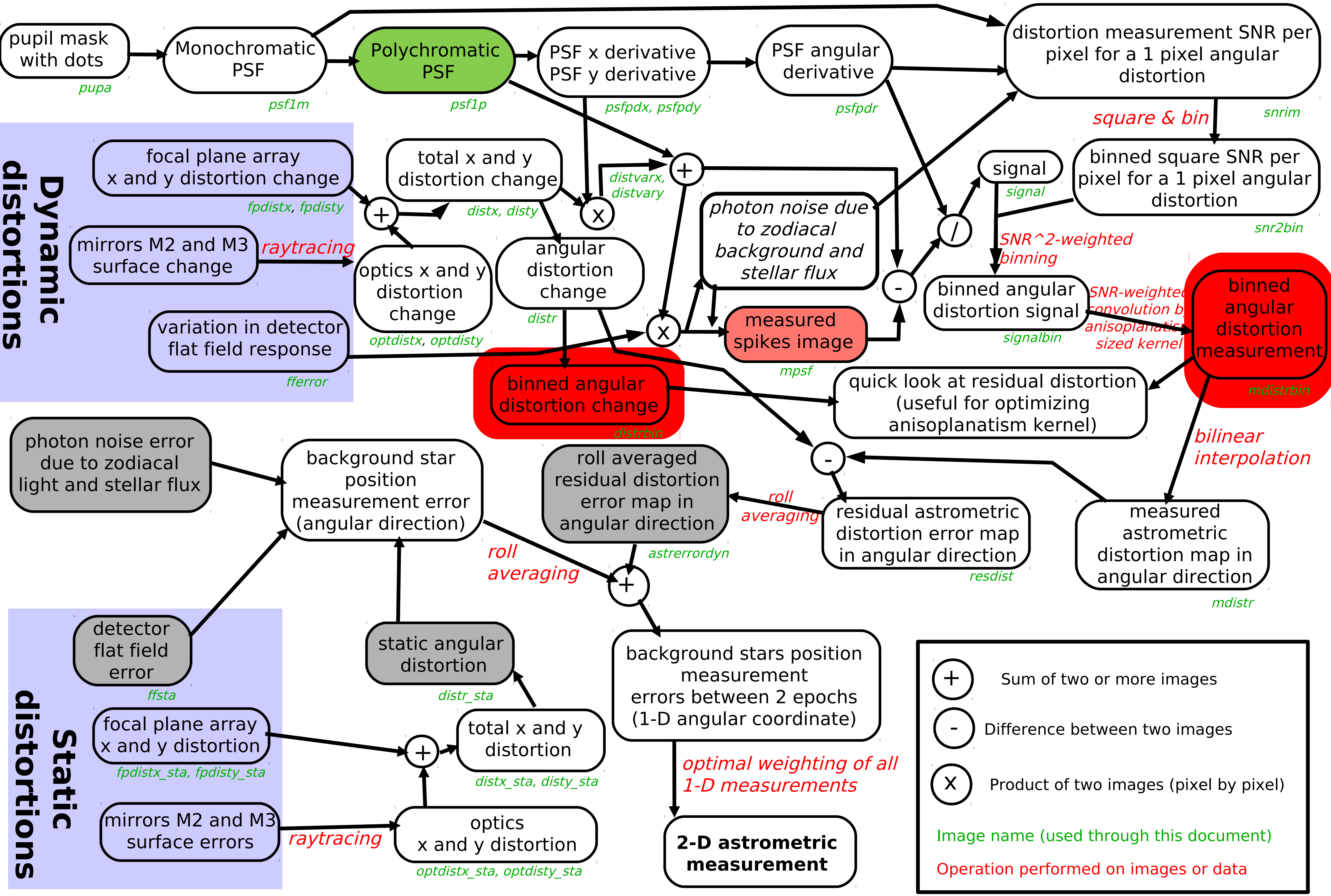

Distortion interpolation

Sigma = 15”

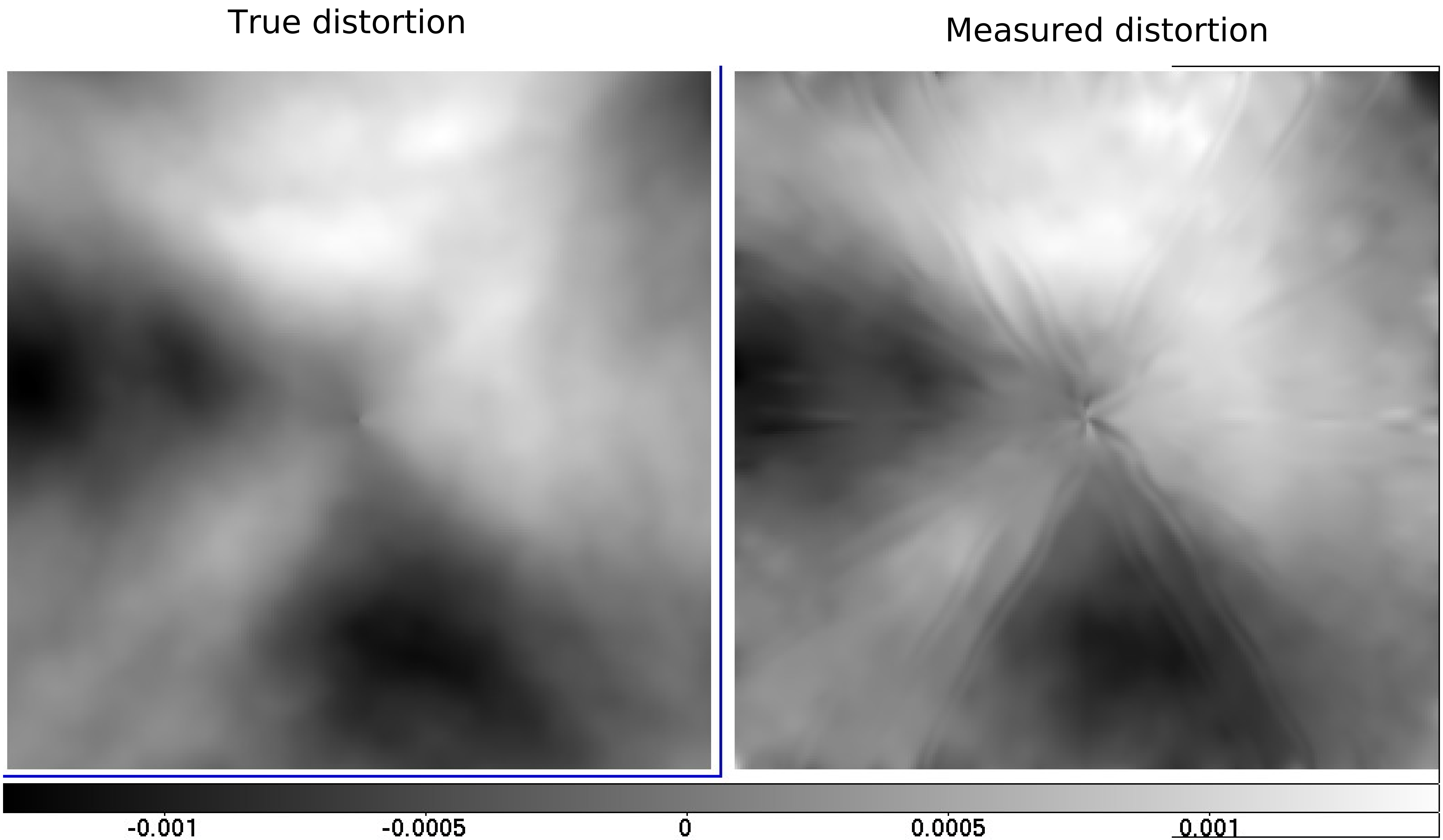

Unit = pixel

Numerical simulation approach

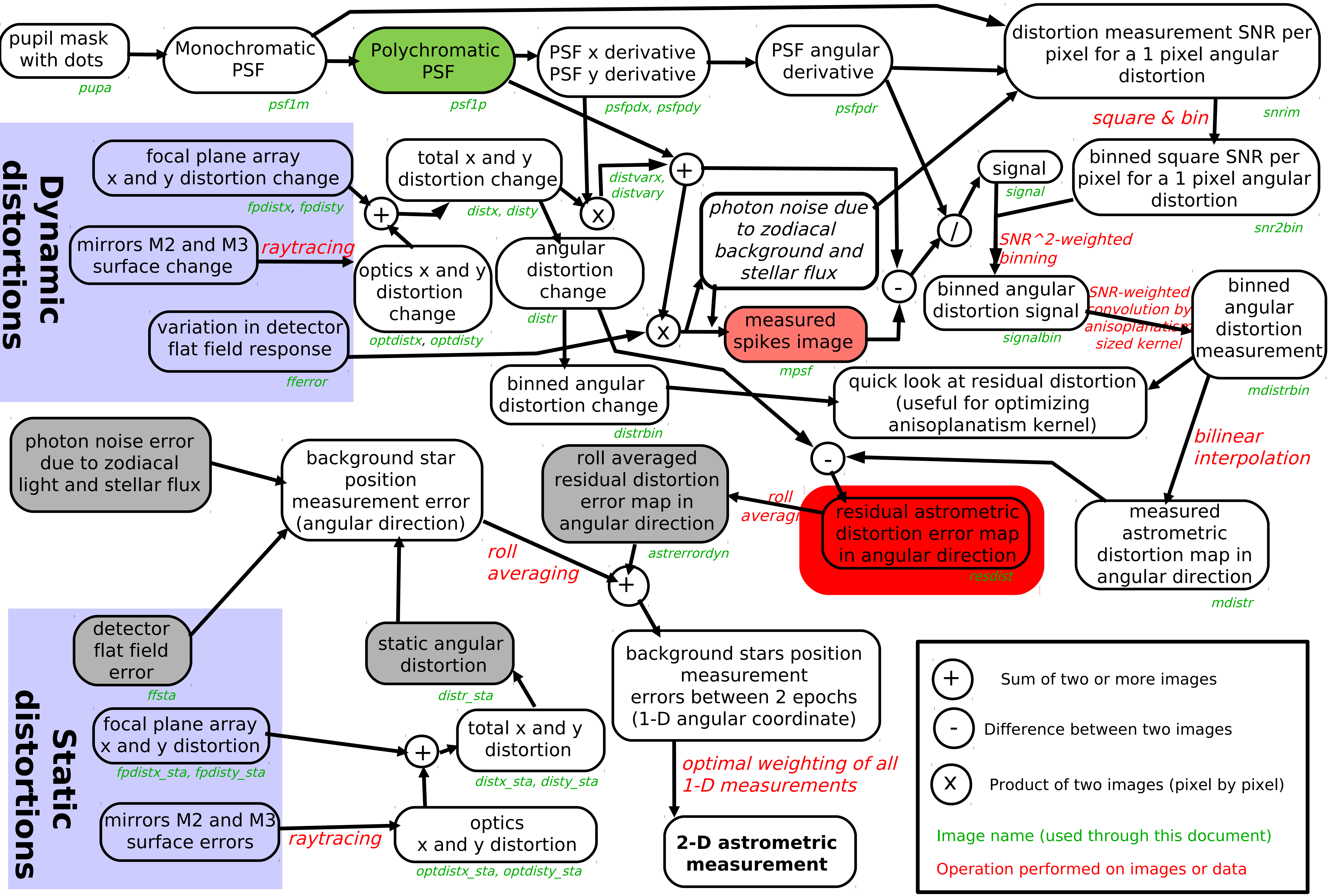

Residual distortion after calibration

Unit = pixel

Residual distortion after calibration is ~1e-4 pix = 4.4 µas
This is 10x smaller than original distortion, and residual is mostly free of low order -> will average well with telescope roll.

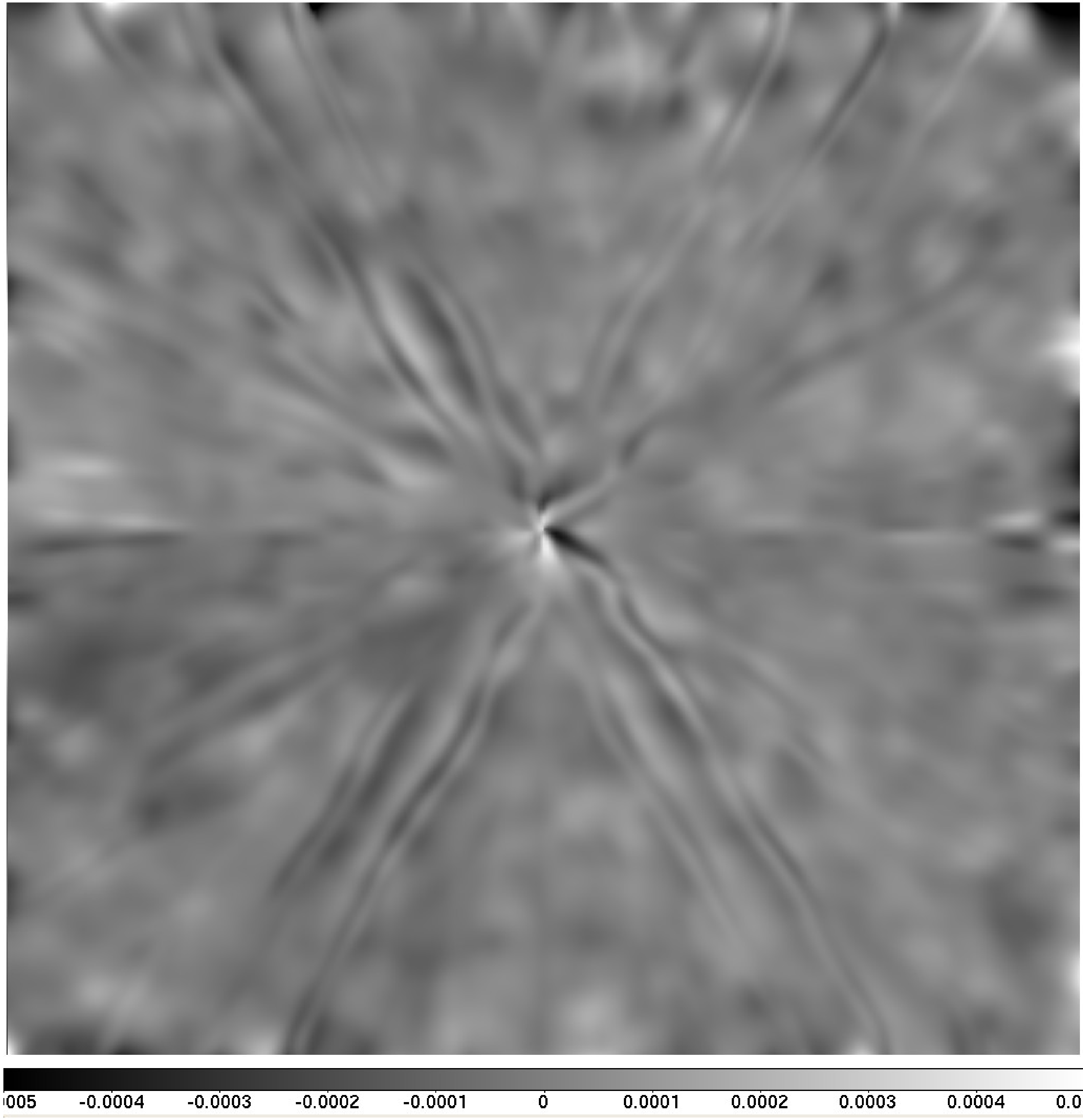

Numerical simulation approach

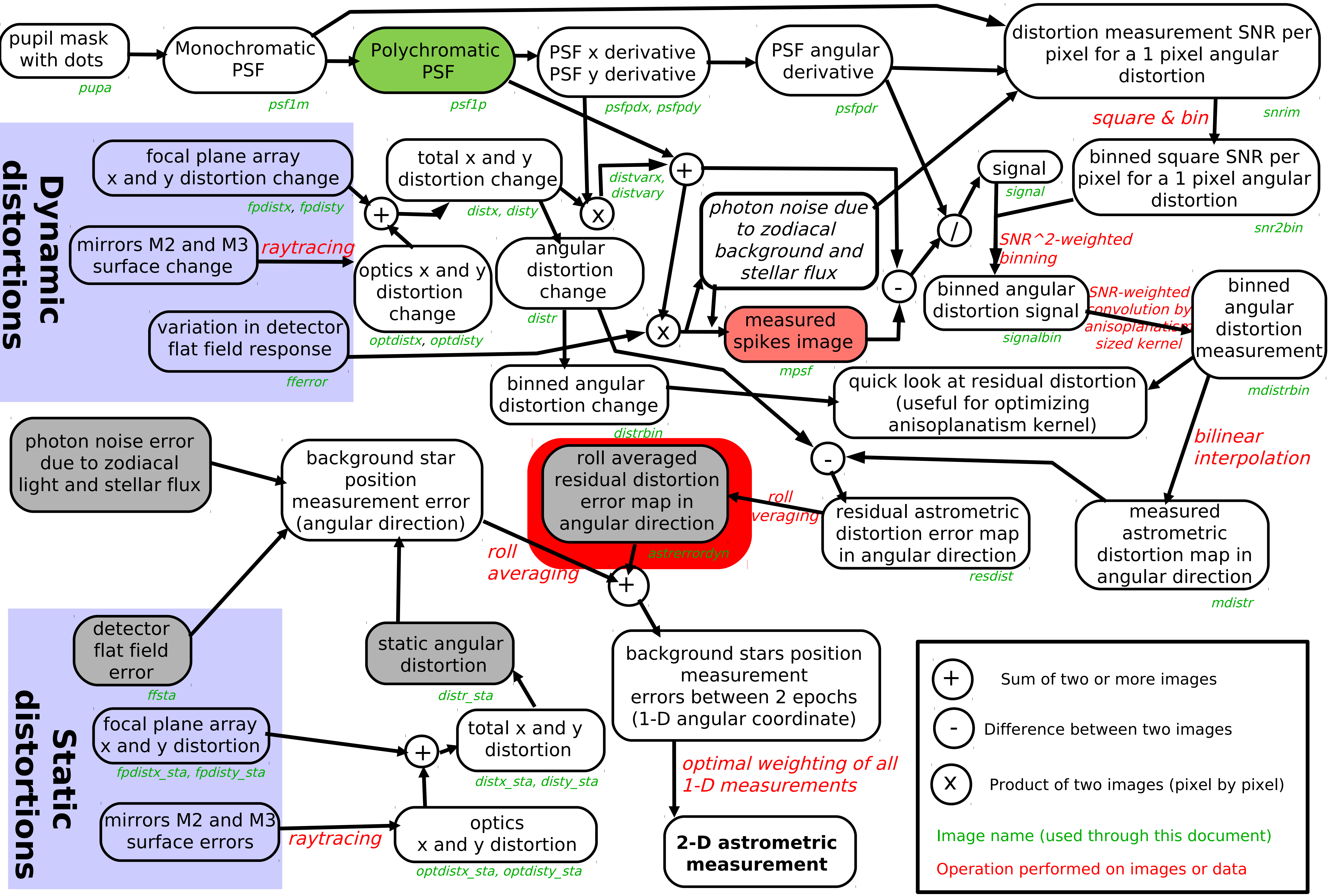

Astrometric error due to distortion changes (after roll)

Unit = arcsec
RMS ~ µas

This map is obtained by roll-averaging the distortion map in the previous slide

Error tends to be smaller for stars further out (more averaging thanks to roll)

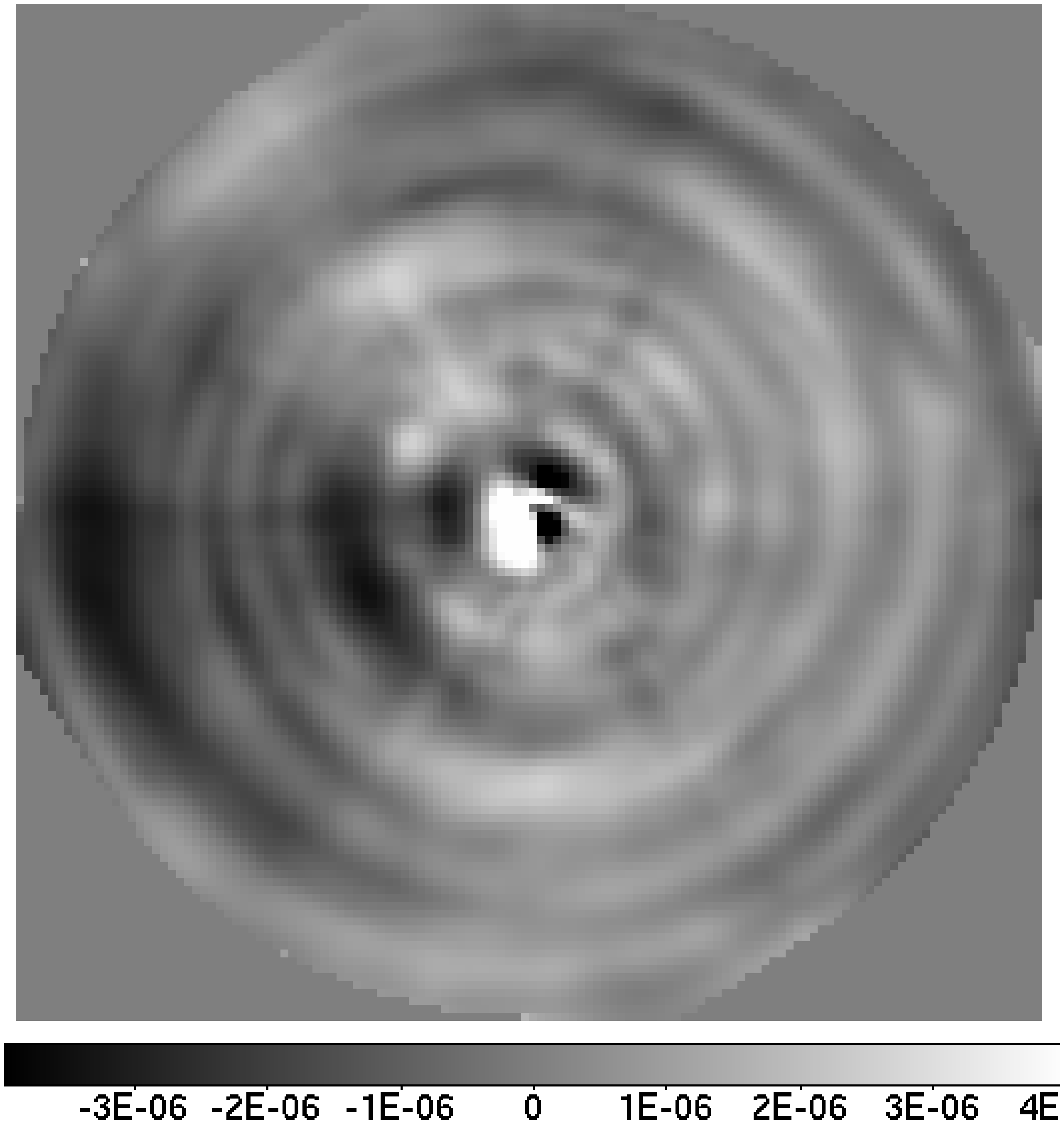

Final astrometric error

For each star, 1-sigma error is computed as quadratic sum of :
- pixel coordinate error (due to photon noise)
- distortion errors (derived from 2D distortion map)
- flat field error on detector

Then, optimally combine all measurement by weighting according to astrometric SNR^2 for each star.

Final astrometric 1 sigma error in this example :
0.58 uas per axis (1-sigma) for 0.03 sq deg (= 0.1 deg radius circular field)

0.2 µas per axis would require 0.25 sq deg (= 0.5 deg x 0.5 deg)
Note: scaling to larger FOV needs to be done more carefully - this is just a rough estimate

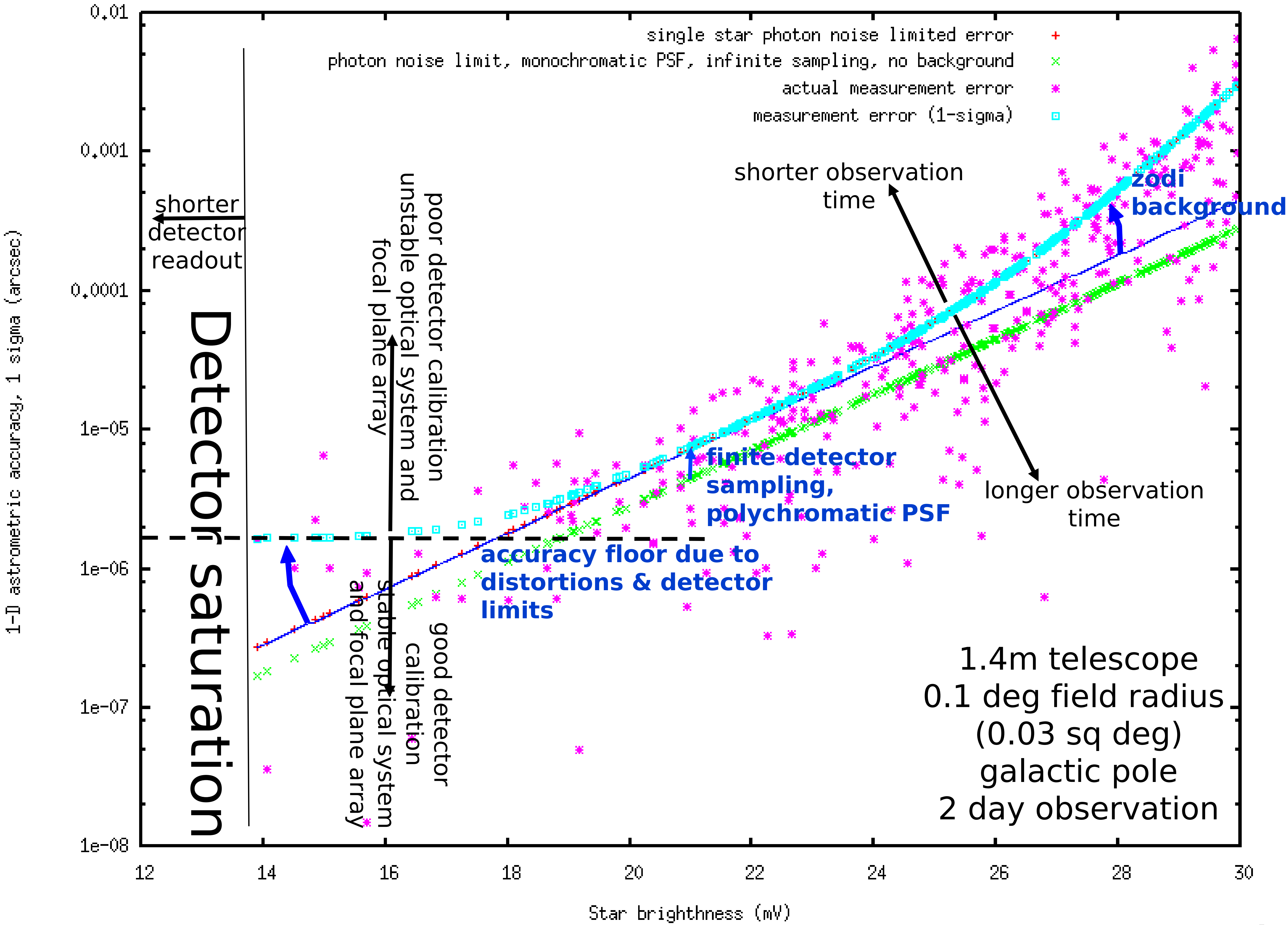
single star photon noise limited error
photon noise limit, monochromatic PSF, infinite sampling, no background
actual measurement error
measurement error (1-sigma)
0.01
0.001
0.0001
1e-05
1e-06
1e-07
1e-08
1-D astrometric accuracy, 1 sigma (arcsec)
12
14
16
18
20
22
24
26
28
30
Star brightness (mV)
shorter detector readout
Detector saturation
poor detector calibration
unstable optical system and focal plane array
good detector calibration
stable optical system and focal plane array
accuracy floor due to distortions & detector limits
finite detector sampling, polychromatic PSF
shorter observation time
longer observation time
zodi background
1.4m telescope
0.1 deg field radius
(0.03 sq deg)
galactic pole
2 day observation